Modeling and Analysis of 100% Renewable Sector-Coupled Energy System for Germany

Md. Nasimul Islam Maruf[1]

Highlights

- An open model approach for analyzing a 100% renewable-based and sector-coupled energy system is proposed.
- An hourly optimization tool based on the open energy modeling framework is developed to investigate the German energy system.
- Scenario results show that a 100% renewable-based system for supplying electricity and building heat is feasible in Germany in 2050 under different conditions.
- Annual investment costs vary between 17.6 – 26.6 bn €/yr for the volatile generators, 23.7 – 28.8 bn €/yr, and a minimum 2.7 – 3.9 bn €/yr for electricity and heat storage.
- Sensitivity analyses show that optimum grid expansion and storage usage storage maximize the flexibility of the system and decrease the overall investment cost.

Abstract

The ambitious energy target to achieve climate-neutrality in the European Union (EU) energy system raises the question of the feasibility of using only renewables across all energy sectors. Germany, as one of the leading industrialized countries of the EU, has adopted several climate action plans for the realistic implementation and maximum utilization of renewable energies in its future energy system. The literature review shows a clear gap in comprehensive techniques describing an open modeling approach for analyzing fully renewable and sector-coupled energy systems. This paper outlines an open modeling technique for analyzing the feasibility of the 100% renewable-based and sector-coupled energy system in Germany. It identifies the capacities and investment costs for different components and briefly evaluates the flexibility aspects of the system in terms of transmission grid expansion, energy storage, and dispatchable loads. Based on the open energy modeling framework (Oemof), an hourly optimization tool 'OSeEM-DE' is developed to investigate the German energy system. The model results show that a 100% renewable-based and sector-coupled system for electricity and building heat is feasible in Germany under different conditions. The investment capacities and component costs depend on the parametric variations of the developed scenarios. According to the model results, the annual investment costs vary between 17.6 – 26.6 bn €/yr for the volatile generators, and between 23.7 – 28.8 bn €/yr for the heat generators. Besides, the model suggests an investment of a minimum of 2.7 – 3.9 bn €/yr for electricity and heat storage. A comparison of the OSeEM-DE results with Fraunhofer ISE study reports shows that the percentage-wise energy mix composition and the Levelized Cost of Electricity (LCOE) from the model are within the plausible ranges. Finally, sensitivity analyses indicate that storage expansion and optimum grid extension between Northern and Southern Germany can maximize the provision of flexibility to the system and decrease the overall investment cost.

Keywords: 100% renewable, energy modeling, energy transition, flexibility, open science, sector coupling.

Broader Context

This research contributes to open energy modeling challenges to analyze 100% renewable-based energy systems for integrated energy sectors. Additionally, it contributes to the studies of renewable energy utilization and the understanding of energy transition in the German context. The research illustrates an in-depth methodology for developing fully renewable and cross-sectoral energy system models and delineates the technique for scenario-based energy system analysis. It advances the understanding of the feasibility of the integrated system and shows the required capacities and investment for its components to stay within the available potentials of renewable resources. The study reveals the possibility of using power-to-heat devices such as electric heat pumps and using biomass-based combined heat and power plants to eliminate the dependency on fossil fuels for heat generation. The study also shows the interrelation between grid and storage

[1]Department of Energy and Environmental Management, Europa-Universität Flensburg, Flensburg, Germany; Postal Address: Auf dem Campus 1b (Room: VIL 108), 24943 Flensburg, Germany; E-mail: ni.maruf@uni-flensburg.de; Phone: +494618053007.

expansion can impact the provision of the flexibility of the energy system. To summarize, the model and the analysis technique will be useful for investigating similar energy systems, especially in the North Sea region.

Nomenclature

Abbreviations

ACAES	Adiabatic Compressed Air Energy Storage
ASHP	Air Source Heat Pump
Capex	Capital Expenditure
CHP	Combined Heat and Power
CSP	Concentrated Solar Power
DE	Germany
Dispa-SET	Unit commitment and optimal dispatch model
DSM	Demand-side Management
ENTSO-e	European Network of Transmission System Operators for Electricity
EU	European Union
FOM	Fixed Operation and Maintenance
GHG	Greenhouse Gas
GSHP	Ground Source Heat Pump
H_2	Hydrogen
LCOE	Levelized Cost of Electricity
Li-ion	Lithium-ion
LP	Linear Programming
MERRA	Modern-Era Retrospective analysis for Research and Application
MILP	Mixed-Integer Linear Programming
NDE	Northern Germany
NPV	Net Present Value
NS	North Sea
O&M	Operation and Maintenance
Oemof	Open Energy Modelling Framework
OPSD	Open Power System Data
OSeEM-DE	Open Sector-coupled Energy Model for Germany
P2H	Power-to-Heat
P2G	Power-to-Gas
PHS	Pumped Hydro Storage
PV	Photovoltaic
PyPSA	Python for Power System Analysis
Redox	Vanadium Redox
ROR	Run-of-the-River
SDE	Southern Germany
TES	Thermal Energy Storage
VOM	Variable Operation and Maintenance
WACC	Weighted Average Cost of Capital
ZNES	Center for Sustainable Energy Systems

Symbols

t	Timestep	T	Set of all timesteps
b	Bus	B	Set of all buses
l	Load	L	Set of all loads
v	Volatile generator	V	Set of all volatile generators
h	Heat pump	H	Set of all heat pumps
s	Storage	S	Set of all storages
m	Transmission line	M	Set of all transmission lines

Variables

$x_{b,in}^{flow}$	Input flow to bus b
$x_{b,out}^{flow}$	Output flow from bus b
x_{l}^{flow}	Load flow of load l
x_{v}^{flow}	Flow of volatile generator unit v
$x_{v}^{capacity}$	Endogenous capacity of volatile generator unit v
$x_{chp}^{flow,carrier}$	Carrier flow of CHP unit chp

$x_{chp}^{flow,electricity}$	Electricity flow of CHP unit chp
$x_{chp}^{flow,heat}$	Heat flow of CHP unit chp
$x_{h,from}^{flow}$	Electricity flow from the electricity bus for heat pump unit h
$x_{h,to}^{flow}$	Heat flow to the heat bus for heat pump unit h
x_{s}^{level}	Energy level of storage unit s
$x_{s,in}^{flow}$	Input flow to storage unit s
$x_{s,out}^{flow}$	Output flow from storage unit s
x_{phs}^{level}	Energy level of pumped hydro storage unit phs
$x_{phs}^{flow,out}$	Output flow of pumped hydro storage unit phs
$x_{phs}^{profile}$	Endogenous inflow profile of pumped hydro storage unit phs
$x_{m,from}^{flow}$	Flow from a bus through the transmission line m
$x_{m,to}^{flow}$	Flow to a bus through the transmission line m

Parameters

$c_{l}^{profile}$	Exogenous profile of load l
c_{l}^{amount}	Total amount of load l
$c_{v}^{profile}$	Exogenous profile of volatile generator v
$c_{v}^{capacity\_potential}$	Maximum capacity potential of volatile generator v
c_{chp}^{beta}	Power loss index of CHP
$c_{chp}^{electrical\_efficiency}$	Electrical efficiency of CHP
$c_{chp}^{thermal\_efficiency}$	Thermal efficiency of CHP
$c_{chp}^{condensing\_efficiency}$	Condensing efficiency of CHP
$c_{biomass}^{amount}$	Absolute amount of biomass commodity
$c_{h}^{efficiency}$	Conversion efficiency (Coefficient of Performance, i.e., COP) of heat pump unit h
$c_{s}^{loss\_rate}$	Loss rate of storage unit s
$c_{s}^{eta\_in}$	Charging efficiency of storage unit s
$c_{s}^{eta\_out}$	Discharging efficiency of storage unit s
$c_{s}^{roundtrip\_efficiency}$	Round Trip efficiency of storage unit s
$c_{s}^{capacity}$	Maximum power capacity of storage unit s
$c_{s}^{storage\_capacity}$	Maximum energy capacity of storage unit s
$c_{phs}^{loss\_rate}$	Loss rate of pumped hydro storage unit phs
$c_{phs}^{efficiency}$	Efficiency of pumped hydro storage unit phs
$c_{phs}^{profile}$	Exogenous inflow profile of pumped hydro storage unit phs
c_{m}^{loss}	Loss on transmission line m
$c^{marginal\_cost}$	Marginal cost
c^{VOM}	Variable operation and maintenance cost
$c^{carrier\_cost}$	Carrier cost
η	Efficiency
$c^{capacity\_cost}$	Capacity cost
$c_{s}^{storage\_capacity\_cost}$	Energy capacity cost of storage
$c^{annuity}$	Annuity cost
c^{capex}	Capital expenditure cost
c^{WACC}	Weighted Average Cost of Capital
c^{FOM}	Fixed operation and maintenance Cost
n	Lifetime
c^{AIV}	Annual investment cost
$c^{optimized\_capacity}$	Optimized capacity cost
c^{TIV}	Total Investment cost
c^{LCOE}	Levelized cost of electricity
I_n	Initial cost of investment expenditure
M_n	Sum of all O&M costs
F_n	Sum of all fuel Costs
E_n	Sum of all electrical energy produced
r	Discount rate

1. Introduction

A clear rulebook was adopted for the practical implementation of the Paris Agreement in December 2018 at the United Nations Climate Conference (COP24) in Katowice, which delineated a world-wide climate action plan to mitigate climate change by reducing global warming to 1.5° C if possible [1]. To achieve a climate-neutral society with net-zero greenhouse gas (GHG) emissions across all sectors by 2050, the European Commission endorsed a strategic long term vision in line with the Paris Agreement for the European Union (EU) [2]. The North Sea (NS) region can be seen as a representative area to demonstrate the feasibility and plausible pathways for achieving the ambitious target of net-zero emission across all the sectors in an energy system [3]. As a leading industrialized nation of the NS region and the EU, Germany already adopted a climate action plan for the realistic implementation of extensive GHG neutrality across all the energy sectors by 2050 [4]. This ambitious energy target requires 'reinvention' of energy systems to be technically feasible and economically viable, guarantying realistic solutions to ensure affordability, reliability, and sustainability [5].

The overcapacity of volatile generators in a 100% renewable-based energy system leads to excess energy in the electricity grid. A relatively new approach known as 'sector coupling' can use this surplus energy efficiently [6]. Sector coupling has emerged as a new concept in energy and climate policy discussions in recent years. The 'Climate Action Plan 2050' and the 'Green Paper on Energy Efficiency' reflect the high political significance of sector coupling, among other things in Germany [4,7]. Sector coupling can make a decisive contribution to the achievement of ambitious climate protection goals through increased use of renewable electricity in the heating and transport sectors and industry to substitute fossil fuels.

The expansion of renewable energies in Germany will increase the need for grid expansion, particularly in local distribution grids for solar photovoltaic (PV) and onshore wind plants, and in the area of transmission grids for offshore wind power. The current power system of Germany has many fossil fuel-based and nuclear-based power plants in Southern Germany. A gradual exit from fossil fuel and nuclear power will require shifting to renewables from offshore wind plants in Northern Germany. Therefore, there will be a need for transmission grid expansion from North to South at the same time. The transmission grid operators and the federal government of Germany have accelerated the development of Grids from Northern to Southern Germany, with 4,650 kilometers to be constructed by 2025 [8]. Figure 1 shows the status of grid expansion in Germany in which the expansion plan from north to south along with other grids in planning and development stages are illustrated [9].

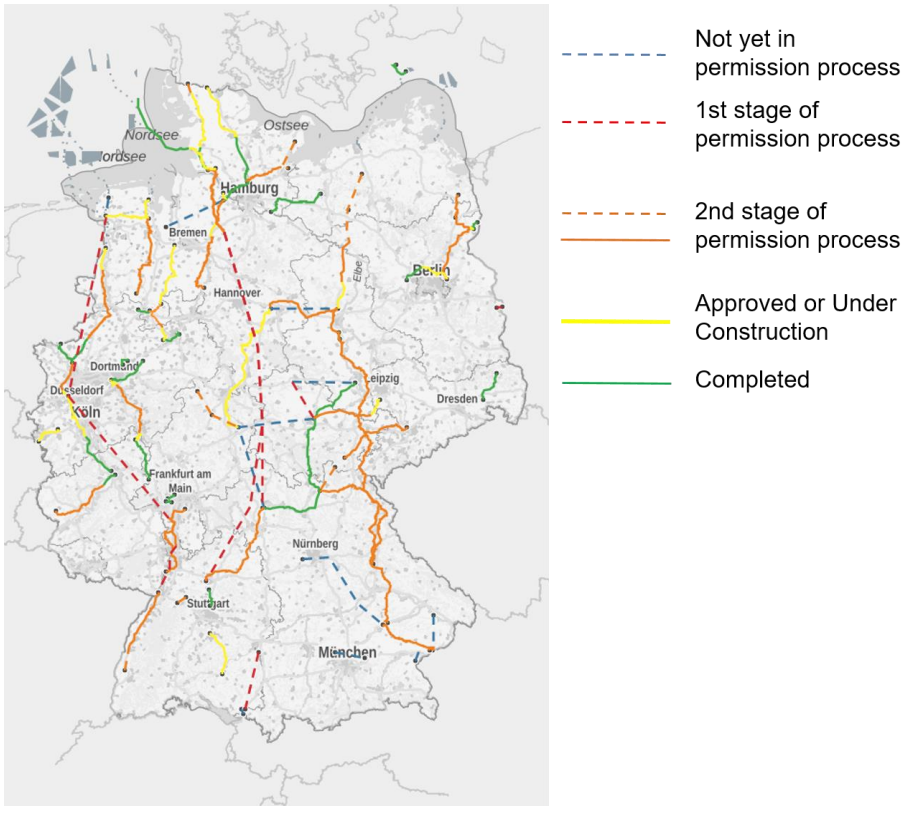

Figure 1: Current status of electricity transmission network planning and development in Germany. The orange, red, and yellow lines show that many North-South grid extension projects are in the planning and development phase. Source: Federal Network Agency of Germany (Bundesnetzagentur) 2020 [9].

Flexibility and sector coupling can bring renewable energies into the various energy sectors in high proportions and raises energy efficiency potentials effectively. By adopting solutions like power-to-heat (P2H) technologies (such as electric heat pumps), and power-to-gas (P2G) technologies (such as Hydrogen storage via electrolysis); the transformation of energy between different energy sectors can be made even more independent of the supply and demand. Flexibility can be offered in various ways, for example, shifting heat pump or electric vehicle loads in private households, and even shifting the energy consumption in industries as a part of an integrated, sector-coupled network. However, the energy flow should be smartly and effectively managed between the sectors to stabilize the network operation while keeping the system flexible and efficient [10].

2. State of the Art and Research Question

In the last two decades, both 'sector coupling' and '100% renewable energy systems' have been subjects of interest for energy researchers globally, as reviewed by the Author in an earlier article [3]. Several pieces of research investigated 100% or near-100% renewable energy systems from the national perspectives. Such investigation includes energy system analysis of Australia, Barbados, Belgium, Brazil, Canada, China, Colombia, Costa Rica, Croatia, Denmark, Finland, France, Germany, Great Britain, Iceland, India and the SAARC region, Iran, Ireland, Italy, Japan, Macedonia, New Zealand, Nigeria, Norway, Pakistan, Paraguay, Portugal, Saudi Arabia, Seychelles, Tokelau, Turkey, Ukraine, the United Kingdom, the United States, and Uruguay [11–52]. Other than these national studies, there are many other 100% renewable system studies larger than national energy systems covering the World, North-East Asia, the ASEAN region, Europe and its neighbors, Europe, South-East Europe, and the Americas [53–66]. Similarly, there are also regional level studies on 100% system for Hvar (Croatia), Mecklenburg-Vorpommern (Germany), Schleswig-Holstein (Germany), Orkney (Scotland), Samsø and many other regions (Denmark), and the Åland Islands (Finland), and the Canary Islands (Spain) [67–70]. Nonetheless, most of these studies focus on 100% renewable-based electricity systems. Only a few consider energy transition pathways for reaching the target, including all the relevant sectors such as heating, cooling, transport, and gas [71].

In German energy system analyses, several studies focus on individual energy sectors such as the heating market, transportation, future electricity market. For achieving the energy transition towards climate-neutrality, Schmid et al. identified and characterized actors who can put the energy transition into practice, but they focused on the power sector only [72]. In a similar publication, Lehmann and Nowakowski analyzed three scenarios for the future electricity system in Germany [73]. Robinius et al. reviewed sector coupling scenarios for Germany linking electricity and transport sectors [6,74]. Gullberg et al. described how the interconnection between Norway and Germany could ensure a low-carbon energy future [75]. Scholz et al. identified the bottlenecks of using only renewables for the energy transition [76]. Schroeder et al. compared different scenarios to investigate the need for grid expansions in Germany [77].

Although there are various modeling and analysis on the German energy transition towards climate neutrality, most of them focus either on specific aspects of an individual energy sector or the markets and actors linked with the energy system. A few studies outline a detailed techno-economic analysis using 100% renewables, including multiple energy sectors in Germany. Palzer and Henning showed that a 100% renewable energy system for power and heat is technically possible, and the overall annual cost for the system will be comparable to today's price. However, their analysis assumes that the building sector, the heat requirement is reduced by 60% in the future compared to today's demand, and their analyzing tool REMod-D is not an open-source model. In another recent publication, Hansen et al. concluded that the full energy system transition towards 100% renewables by 2050 in Germany is technically and economically possible, but resource potentials, mainly biomass, is a big challenge for this transition. Hansen et al. used EnergyPLAN for their analysis, a popular free-to-use simulation tool for modeling 100% systems for all energy sectors. However, it is not possible to analyze the capacity expansion mechanism and reach an optimum solution using EnergyPLAN [78]. A literature review by Maruf shows that there is a clear research gap in applying cross-sectoral holistic approaches using comprehensive open modeling techniques for analyzing 100% renewable and sector-coupled models in Germany and the other countries in the NS region [3]. Therefore, based on the scope of further research on this subject, the following research question is formulated–

How feasible is it to transform towards a 100% renewable energy system for both power and heat sectors in Germany by 2050?

Answering the main research question raises additional questions on the overall energy mix, investment cost and capacities, the issue of grid expansion within Germany, and different flexibility aspects of the system; which formulates the following sub-research questions–

1. *In which capacities such a system can be implemented?*
2. *What are the estimated investment costs for the different system components?*
3. *What are the flexibility aspects of grid expansion, storages, and dispatchable loads in such a system?*

The main objective of the paper is to design, develop, and investigate an open-source energy model for Germany for both power and heat sectors. The model analyzes different scenarios to investigate moderate to extreme conditions to determine the plausible energy mix and required investment in component-wise capacities and costs. The model considers dividing the German energy system into two sub-national regions so that the grid expansion from Northern to Southern Germany can be analyzed. It also helps to understand the underlying energy flow mechanism and the role of different energy components from both national and sub-national perspectives. The analysis of the heating sector in this model is limited to the use of building heat, including space heating and domestic hot water demands. The study does not consider the inclusion of industrial process heating demands using renewables.

Section 3 describes the methodology of the model, which consists of the architecture of the model and its component-wise mathematical description. Section 4 describes the details of the working mechanism of the developed model and the input data used for the analysis. Section 5 describes the development of different scenarios. Section 6 presents and compares the scenario results and examines the details of the system based on the research questions. Section 7 summarizes the results and concludes with the future steps of the research.

3. Methodology

The optimization model follows a hybrid approach where the current technology capacities are exogenously defined, and the future investment capacities are endogenously determined. System boundaries, according to technology potentials, are set to avoid any unrealistic solution based on overestimation. The 'Open Sector-coupled Energy Model for Germany (OSeEM-DE)' is an application constructed using 'Oemof Tabular'-python-based linear programming (LP) optimization tool under the open energy modeling framework (Oemof) [79]. As shown in Figure 2, the two German sub-national energy system nodes are Northern Germany (NDE) and Southern Germany (SDE). NDE consists of Schleswig-Holstein, Lower Saxony, Bremen, Hamburg, and Mecklenburg-Vorpommern, and SDE consists of the remaining eleven states of Germany. The power exchange between NDE and SDE is possible using the transshipment approach via NDE-SDE Link.

Figure 2: The German national energy system with two sub-national nodes, NDE (shown using blue color) and SDE (shown using green color). Map source: Wikimedia Commons [80].

Figure 3 illustrates the Oemof-based OSeEM-DE energy system model. The volatile components of the model are onshore wind, offshore wind, Solar Photovoltaic, and hydro Run-of-the-River (ROR) plants. The fuel input of the Combined Heat and Power (CHP) plants comes from biomass resources. Besides CHP, Air Source Heat Pump (ASHP) and Ground Source Heat Pump (GSHP) can generate heat. The storage options are Pumped Hydro Storage (PHS), Lithium-ion (Li-ion) battery, Vanadium Redox (Redox) flow battery, Hydrogen (H_2) storage, and Adiabatic Compressed Air Energy Storage (ACAES). The heat storage option is Thermal Energy

Storage (TES) using hot water tanks. NDE and SDE energy systems are almost identical, except that offshore wind and ACAES components are only available in NDE.

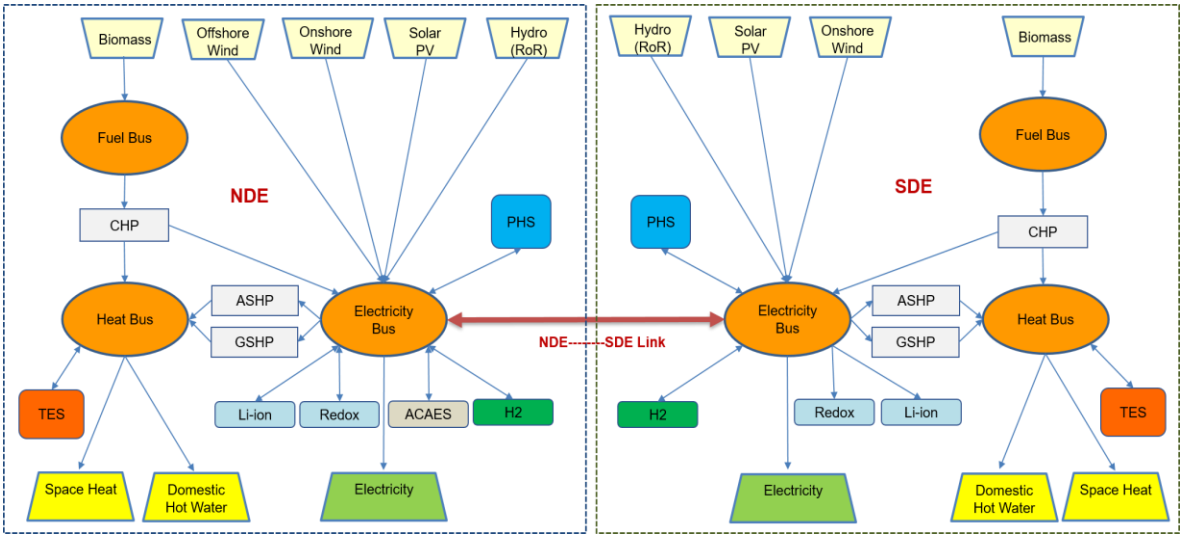

Figure 3: Simplified block diagram of the Oemof-based OSeEM-DE model for Germany showing NDE and SDE nodes.

The OSeEM-DE model follows the formulation methodology using Oemof Solph described by Hilpert, where the maximum potential constrains the volatile renewable sources, total biomass amount, and storage capacities [81]. The transmission capacity between NDE and SDE and the heat storage capacities are also limited exogenously. The upper limit for the P2H technologies are subject to optimization but depends on the availability of electricity. The different components of the energy system and their mathematical formulations are as follows, where x denotes the endogenous variables, and c denotes the exogenous parameters used in the model.

3.1. Bus

There are three types of buses in the energy model: electrical, heat, and fuel bus. Since all flows into and out of a bus are balanced, for the set of all buses $b \in B$, sum of all input flows $x_{b,in}^{flow}$ to a bus b must be equal to the sum of all output flows $x_{b,out}^{flow}$:

$$\sum x_{b,in}^{flow}(t) = \sum x_{b,out}^{flow}(t) \qquad \forall t \in T, \forall b \in B \tag{1}$$

3.2. Load

Two types of loads are considered in the energy model: electricity and heat. The heat load consists of space heat and domestic hot water. For the set of all loads $l \in L$, the load flow x_l^{flow} at every time step t must be equal to the product of two exogenously given inputs: profile value of the load $c_l^{profile}$ at time step t, and the total amount of the load c_l^{amount}:

$$x_l^{flow}(t) = c_l^{profile}(t) \,.\, c_l^{amount} \qquad \forall t \in T, \forall l \in L \tag{2}$$

3.3. Volatile Generator

The volatile generators in the model are onshore and offshore wind, solar PV, and hydro ROR plants. These components are connected to electricity buses. The offshore wind component is available only in NDE. For all the volatile generators $v \in V$, the flow x_v^{flow} at every time step t must be equal to the product of the capacity $x_v^{capacity}$ and the profile value of the volatile generator $c_v^{profile}$:

$$x_v^{flow}(t) = x_v^{capacity}(t).\, c_v^{profile}(t) \qquad \forall t \in T, \forall v \in V \tag{3}$$

The endogenously obtained capacity of the generator $x_v^{capacity}$ at every time step t must be less than or equal to the maximum capacity potential of the volatile component $c_v^{capacity\_potential}$:

$$x_v^{capacity}(t) \leq c_v^{capacity\_potential} \qquad \forall t \in T, \forall v \in V \tag{4}$$

3.4. Combined Heat and Power (CHP)

Since the model is 100% RES-based, the CHP plants use only biomass resources as fuel. Thus, biomass goes into the fuel bus, which later goes as the input of CHP, as shown in Figure 3. The CHP runs in extraction turbine mode, as shown by (5 – 7), according to Mollenhauer et al. [82]. (5) shows the relation between the input carrier flow $x_{chp,}^{flow,carrier}$ and the two output flows: electrical output flow $x_{chp}^{flow,electricity}$ and heat output flow $x_{chp}^{flow,heat}$, at every time step t. (6) shows the relationship between the two output flows. c_{chp}^{beta} is the power loss index, which is derived using (7). $c_{chp}^{electrical\_efficiency}$, $c_{chp}^{thermal\_efficiency}$ and $c_{chp}^{condensing\_efficiency}$ denote the electrical, thermal and condensing efficiencies of the CHP unit, respectively.

$$x_{chp}^{flow,carrier}(t) = \frac{x_{chp}^{flow,electricity}(t) + x_{chp}^{flow,heat}(t) \,.\, c_{chp}^{beta}}{c_{chp}^{condensing\_efficiency}} \qquad \forall t \in T \tag{5}$$

$$x_{chp}^{flow,electricity}(t) \geq x_{chp}^{flow,heat}(t) . \frac{c_{chp}^{electrical\_efficiency}}{c_{chp}^{thermal\_efficiency}} \qquad \forall t \in T \tag{6}$$

$$c_{chp}^{beta} = \frac{c_{chp}^{condensing\_efficiency} - c_{chp}^{electrical\_efficiency}}{c_{chp}^{thermal\_efficiency}} \tag{7}$$

Equation (8) models the limited availability of biomass commodities where the aggregated inflows are constrained by the absolute amount of the biomass commodity $c_{biomass}^{amount}$:

$$\sum x_{chp}^{flow,carrier}(t) \leq c_{biomass}^{amount} \qquad \forall t \in T \tag{8}$$

3.5. Heat Pump

In addition to CHPs, two types of heat pumps are used to supply heat loads in the model: ASHP and GSHP, the latter being the more efficient but expensive option. Oemof Solph's conversion component, which converts power to heat, is used for modeling both heat pumps. Therefore, a conversion process of one input flow $x_{h,from}^{flow}$ (electricity flow from the electricity bus) and one output $x_{h,to}^{flow}$ (heat flow to the heat bus) and a conversion factor $c_{h,to}^{efficiency}$ (conversion efficiency i.e., coefficient of performance of the heat pump) at every time step t models all the heat pumps $h \in H$:

$$x_{h,to}^{flow}(t) = x_{h,from}^{flow}(t) . c_{h,to}^{efficiency} \qquad \forall t \in T, \forall h \in H \tag{9}$$

3.6. Storage

In addition to PHS, the other electricity storage technologies used in the model are Li-ion and Redox batteries, ACAES, and H_2 storage. Hot water-based TES is the only heat storage component in both NDE and SDE. Oemof Solph's generic storage formulations are used to model all the storage components except PHS. For all these storages $s \in S$, the mathematical model includes the input and output flows and the storage level:

$$x_s^{level}(t) = x_s^{level}(t-1) . \left(1 - c_s^{loss\_rate}\right) + c_s^{eta\_in} . \, x_s^{flow,in}(t) - \frac{x_s^{flow,out}(t)}{c_s^{eta\_out}} \qquad \forall t \in T, \forall s \in S \tag{10}$$

Where x_s^{level} indicates the storage energy level, $c_s^{loss\_rate}$ marks the loss rate for the storage, $x_s^{flow,in}$ and $x_s^{flow,out}$ indicates the input and output flows, and $c_s^{eta\_in}$ and $c_s^{eta\_out}$ denotes the charging and discharging efficiencies of the storage.

The charging and discharging efficiency is formulated from the roundtrip efficiency using $c_s^{eta} = \sqrt{c_s^{roundtrip\_efficiency}}$. The input and output flows x_s^{flow} are constrained by the maximum power capacity

$c_s^{capacity}$ as shown in (11). The energy level x_s^{level} is constrained by the maximum energy capacity $c_s^{storage\_capacity}$ as shown in (12).

$$x_s^{flow}(t) \leq c_s^{capacity} \quad \forall t \in T, \forall s \in S \tag{11}$$

$$x_s^{flow}(t) \leq c_s^{storage\_capacity} \quad \forall t \in T, \forall s \in S \tag{12}$$

3.7. Pumped Hydro Storage

The PHS are modeled as storage units with a constant inflow and possible spillage:

$$x_{phs}^{level}(t) = x_{phs}^{level}(t-1).\left(1 - c_{phs}^{loss\_rate}\right) + x_{phs}^{profile}(t) - \frac{x_{phs}^{flow,out}(t)}{c_{phs}^{efficiency}} \quad \forall t \in T \tag{13}$$

Where x_{phs}^{level} indicates the pumped hydro storage energy level, $c_{phs}^{loss\_rate}$ marks the loss rate for the PHS, $x_{phs}^{profile}$ indicates the endogenous inflow profile, $x_{phs}^{flow,out}$ denotes the output flow from the PHS, and $c_{phs}^{efficiency}$ marks the efficiency of the PHS. The hydro inflow is constrained by an exogenous inflow profile:

$$0 \leq x_{phs}^{profile}(t) \leq c_{phs}^{profile}(t) \quad \forall t \in T \tag{14}$$

Therefore, if the inflow exceeds the maximum storage capacity, spillage is possible by setting $x_{phs}^{profile}$ to lower values. The spillage at time step t can therefore be defined by $c_{phs}^{profile}(t) - x_{phs}^{profile}(t)$.

3.8. Transmission Line

The electricity transmission between two energy systems via NDE-SDE Link is modeled using the transshipment approach, which facilitates simple electricity exchange (import-export) after considering a transmission loss factor. Therefore, transmission lines $m \in M$ are modeled according to the following mathematical formulation:

$$x_{m,from}^{flow}(t) = (1 - c_m^{loss}).x_{m,to}^{flow}(t) \quad \forall t \in T, \forall m \in M \tag{15}$$

Where $x_{from,m}^{flow}$ indicates the flow from the supplying energy system, $x_{m,to}^{flow}$ indicates the flow to the receiving energy system, and c_m^{loss} indicates the loss on transmission line m.

3.9. Costs

The marginal costs $c_{v,chp,h,s}^{marginal\_cost}$ are calculated based on the variable operation and maintenance (VOM) cost $c_{v,chp,h,s}^{VOM}$, carrier cost $c_{v,chp,h,s}^{carrier\_cost}$, and the efficiency of the corresponding technology $\eta_{v,chp,h,s}$:

$$c_{v,chp,h,s}^{marginal\_cost} = c_{v,chp,h,s}^{VOM} + \frac{c_{v,chp,h,s}^{carrier\_cost}}{\eta_{v,chp,h,s}} \tag{16}$$

The capacity costs for volatile generators, CHP and heat pumps $c_{v,chp,h}^{capacity\_cost}$ are calculated based on the fixed operation and maintenance (FOM) cost $c_{v,chp,h}^{FOM}$, and the annuity of the corresponding technology $c_{v,chp,h}^{annuity}$, as shown in (17). The annuity $c^{annuity}$ is calculated using (18), which consist of the initial capital expenditure c^{capex}, the weighted average cost of capital c^{WACC}, and the lifetime of the investment n for the respective technology.

$$c_{v,chp,h}^{capacity\_cost} = c_{v,chp,h}^{FOM} + c_{v,chp,h}^{annuity} \tag{17}$$

$$c^{annuity} = c^{capex}.\frac{(c^{WACC}.(1 + c^{WACC})^n}{((1 + c^{WACC})^n - 1)} \tag{18}$$

In the case of storages, the capacity costs $c_s^{capacity\_cost}$ and the storage capacity costs $c_s^{storage\_capacity\_cost}$ are calculated using (19 – 20):

$$c_s^{capacity\_cost} = c_{s,power}^{annuity} \quad (19)$$

$$c_s^{storage\_capacity\_cost} = c_s^{FOM} + c_{s,energy}^{annuity} \quad (20)$$

Where, $c_{s,power}^{annuity}$ is the annuity cost of storage power , and $c_{s,energy}^{annuity}$ is the annuity cost of storage energy. These two annuities are calculated using the formulation of (18). c_s^{FOM} is the fixed operation and maintenance cost (FOM) of energy storage.

In addition to these modeling equations, some costs are calculated and analyzed after a successful model run, based on the optimization results. The annual investment cost c^{AIV} is calculated multiplying the annuity $c^{annuity}$ and the optimized capacity $c^{optimized\_capacity}$, as shown in (21). The total investment (overnight) investment cost c^{TIV} is calculated multiplying the capital expenditure c^{capex}, and the optimized capacity $c^{optimized\_capacity}$, as shown in (22). Furthermore, the Levelized Costs of Electricity c^{LCOE} is calculated from the ratio of the Net Present Value (NPV) of total costs of over lifetime (including fixed and variable operation and maintenance costs, fuel costs, and the discount rate), and the NPV of the electrical energy produced over the lifetime, as shown in (23).

$$c^{AIV} = c^{annuity} . c^{optimized\_capacity} \quad (21)$$

$$c^{TIV} = c^{capex} . c^{optimized\_capacity} \quad (22)$$

$$c^{LCOE} = \frac{\sum \frac{(I_n + M_n + F_n)}{(1+r)^n}}{\sum \frac{E_n}{(1+r)^n}} \quad (23)$$

Where I_n indicates the initial cost of investment expenditures (same as c^{capex}), M_n indicates the sum of all operation and maintenance expenditures (sum of c^{VOM} and c^{FOM}), and F_n indicates the fuel expenditure (such as the carrier cost of biomass), E_n indicates the sum of all electrical energy generation, r indicates the discount rate (same as c^{WACC}), and n indicates the lifetime.

3.10. Objective Function

The objective function is created from all instantiated objects which use all operating costs and investment costs arguments:

$$\begin{aligned} min: & \sum_{v,t} \overbrace{x_v^{flow}(t).c_v^{marginal\_cost}}^{operating\_cost\ Volatile\ Generator} + \sum_{v} \overbrace{x_v^{capacity}.c_v^{capacity\_cost}}^{investment\_cost\ Volatile\ Generator} + \\ & \sum_{chp,t} \overbrace{x_{chp}^{flow}(t).c_{chp}^{marginal\_cost}}^{operating\_cost\ CHP} + \sum_{chp} \overbrace{x_{chp}^{capacity}.c_{chp}^{capacity\_cost}}^{investment\ cost\_CHP} + \\ & \sum_{h,t} \overbrace{x_h^{flow}(t).c_h^{marginal\_cost}}^{operating\_cost\ Heat\ Pump} + \sum_{h} \overbrace{x_h^{capacity}.c_h^{capacity\_cost}}^{investment\_cost\ Heat\ Pump} + \\ & \sum_{s,t} \overbrace{x_s^{flow}(t).c_s^{marginal\_cost}}^{operating\_cost\ Storage} + \\ & \sum_{s} \overbrace{x_s^{capacity}.c_s^{capacity\_cost} + x_s^{storage\_capacity}.c_s^{storage\_capacity\_cost}}^{investment\_cost\ Storage} \end{aligned} \quad (24)$$

4. Model

The underlying concept of the OSeEM-DE model uses the formulation of LP and mixed-integer linear programming (MILP) from a generic object-oriented structure of Oemof Solph, which allows creating models on different levels of detail using predefined components and an optional formulation of expressions and constraints. Figure 4 shows a summary of the OSeEM-DE model input and output.

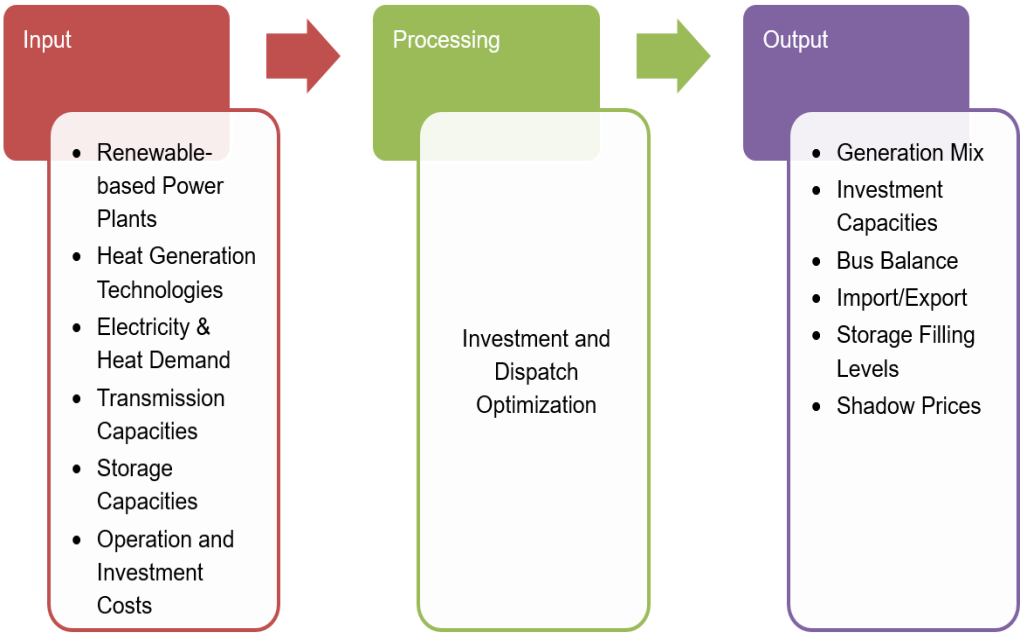

Figure 4: Input and output of the OSeEM-DE model

The input data used in the model are the capacities and potentials of renewable energy-based power plants (such as wind, PV), heat generation technologies (such as CHP, heat pump), electricity and heat demands, transshipment capacity, storage capacities, and their potential. Also, operating costs (i.e., marginal cost) and the investment costs (i.e., capacity cost) for all the considered technologies are provided as input. After solving the model using open model solvers, the results are post-processed using Oemof Tabular's post-processing scripts. The output of the model provides information on the generation mix, investment capacities according to the provided capacities and available potential, balance in each of the buses, import/export between energy systems (in this case between NDE and SDE), filling level of the storages and the shadow prices.

Python language is used for scripting the model according to the flowchart shown in Figure 5. After starting the necessary packages (such as pandas, facades, post-processing), input data, and result directories are set up, and input data are read from external .csv files. Different scenarios are built in this stage with different datasets, which are further discussed in the scenario development part of this paper. The input datasets are pre-processed before importing them to the input .csv files. After the input dataset is read, the energy system is created, and different buses are created and added to the energy system using Oemof Solph. Then different components (such as power, heat, and storage components) are added to the energy system from Oemof Tabular's 'Facades' classes. Then the energy model is created and solved using Oemof Solph. After successful optimization, results are post-processed and written to several .csv files using Oemof Tabular's post-processing tool, which are later illustrated using Oemof Tabular's 'Plots' tool.

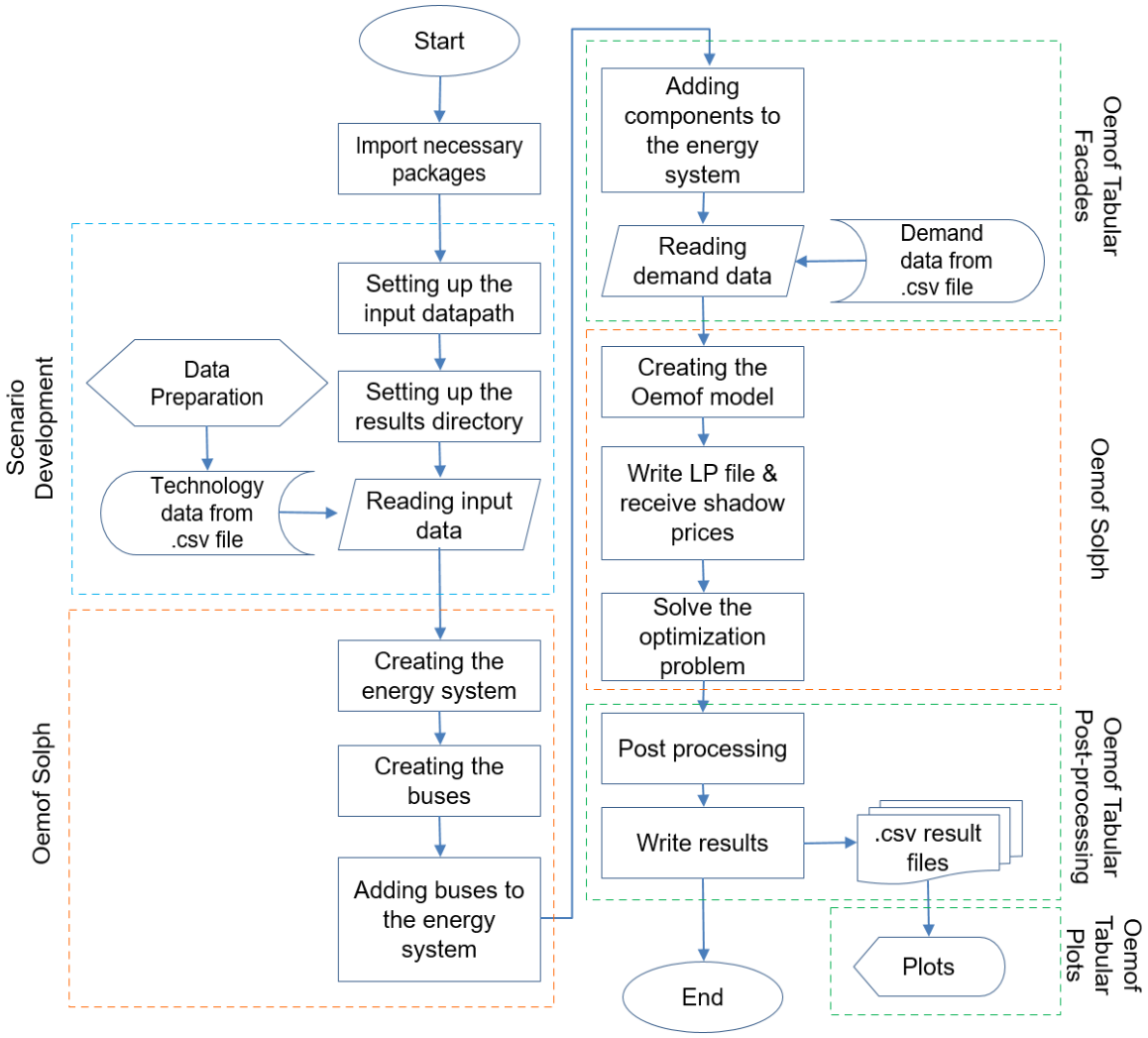

Figure 5: OSeEM-DE Model development

4.1 Input Data: Hourly Profiles and Capacities

The model optimizes investment and operation for a full year of historical hourly data, with 2011 chosen as the primary representative year because of its average wind conditions, high solar irradiation (representing the expected warm condition in 2050 due to the climate change), slightly lower overall heating demand, and duration of maximum heating demand during the wintery days [83].

4.1.1. Electricity and Heat Load

The hourly electricity load data based on the *ENTSO-e* statistical database are obtained from the *Open Power System Data (OPSD) Project* [84,85]. Hourly normalized time series are obtained from the electricity load data for both NDE and SDE energy systems based on population-based clustering. The total electricity demand for Germany in 2050, based on the representative year, is 532.77 TWh_{el}, of which NDE accounts for 96.6 TWh_{el}, and SDE accounts for 436.16 TWh_{el}.

The hourly heat load data based on the *When2Heat Project* are obtained from the *OPSD Project* database [84,86,87]. Heat demand time series for space heat and hot water for Germany are obtained separately from the *When2Heat* profiles and are clustered and normalized for use as inputs of the model. The total heat demand for Germany in 2050, based on the representative year, is 648.53 TWh_{th}. Total space heating demand accounts for 533.6 $TWh_{th,}$ of which NDE accounts for 96.75 TWh_{th}, and SDE accounts for 436.85 TWh_{th}. Total hot water demand accounts for 114.92 $TWh_{th,}$ of which NDE accounts for 20.83 TWh_{th}, and SDE accounts for 94.08 TWh_{th}.

4.1.2. Volatile Generator

Normalized onshore wind profiles based on *MERRA-2* datasets are obtained separately for NDE and SDE energy systems from the *Renewables Ninja Project*. Normalized offshore wind profiles based on *MERRA-2* datasets are also obtained from the *Renewables Ninja Project*. Similarly, normalized solar PV profiles based

on *MERRA-2* datasets are obtained separately for NDE and SDE energy systems from the *Renewables Ninja Project* [88]. Hydro inflow data for the ROR plants are obtained and normalized from the *Dispa-SET Project* database [89]. The current capacity and potential data are obtained or calculated from the *Agency for Renewable Energies*, *Deutsche WindGuard*, *Limes-EU Project*, *ZNES*, *ANGUS II Project*, and *PyPSA Project* databases [90–97]. Table 1 shows the capacity and available potential data for the volatile generators in 2050.

Table 1. Capacity and potential for volatile generators in the German energy system in 2050

Energy System		**Onshore Wind [GW_{el}]**	**Offshore Wind [GW_{el}]**	**Solar PV [GW_{el}]**	**Hydro ROR [GW_{el}]**
NDE	Capacity	22.12	6.66	7.56	0.09
	Available Potential	49.88	76.94	55.77	0.06
SDE	Capacity	31.79	-	37.66	4.2
	Available Potential	118.81	-	188.07	1.1
Germany	Total Capacity	53.91	6.66	45.23	4.29
	Total Available Potential	168.69	76.94	243.84	1.16

4.1.3. CHP and Heat Pump

The amount of available biomass is calculated from the data available from the *Hotmaps Project* for forest residues, livestock effluents, and agricultural residues [98]. According to the calculation for a full year, the available potential for biomass in NDE is 141.1 PJ, and in SDE, it is 493.23 PJ, totaling 634.33 PJ for the whole of Germany. For the current capacities, it is assumed that the existing biomass and biogas-based power plants are converted to CHP plants by 2050. Therefore, 4.74 GW CHP in NDE and 8.86 GW CHP in SDE energy systems are assumed to be installed and fully operational by 2050. The current heat pump capacities are considered zero, and their investment potentials are not constrained. However, since heat pumps are P2H devices, their investment capacities depend upon limited available power from the potentially constrained volatile generators.

4.1.4. Storage

The capacity and available maximum potential data for storage investments are described in Table 2. Data for Li-ion and Redox flow batteries, H_2 storages, and ACAES are obtained from the *ANGUS II Project* scenarios for Germany in 2050 [97]. PHS data are obtained from the *Dispa-SET Project* dataset [89]. For batteries, H_2 storage, and TES, it is assumed that 18% of the total potential of Germany is available for NDE, and the rest is available for SDE.

Table 2. Capacity and maximum potential for storage investments

Energy System		**Li-ion [GW_{el}]**	**Redox [GW_{el}]**	**Hydrogen [GW_{el}]**	**ACAES [GW_{el}]**	**PHS [GW_{el}]**	**TES* [GW_{th}]**
NDE	Capacity	0	0	0	0.29	0.34	0
	Available Potential	2.82	0.17	1.82	3.43	-	1.8
SDE	Capacity	0	0	0	-	0.82	0
	Available Potential	12.83	0.76	8.28	-	-	8.2
Germany	Capacity	0	0	0	0.29	8.57	0
	Available Potential	15.65	0.93	10.1	3.43	-	10

*Own assumption

The energy storage potentials for the batteries, H_2 storage, and ACAES investment are subject to optimization. The storage potential for the existing ACAES plant in Huntorf is 0.58 GWh_{el} [99]. Inflow data for PHS are derived from the *Dispa-SET Project*'s scaled inflow dataset and the current PHS capacity of Germany. Storage

capacities for PHS are taken from the *Dispa-SET Project* dataset, which is 1.7 GWh_{el} for NDE, and 717 GWh_{el} for SDE [89]. PHS investment is excluded because of the limited expansion capacity. A loss rate of 1% for PHS and 1.4% for TES are considered in the model [83,89,97].

4.1.5 Transmission Line

The transmission lines in between NDE and SDE energy systems (NDE-SDE Link) are modeled as transshipment capacities with line loss. The total transmission capacity is set and varied exogenously for different scenarios. A line loss of 4% is considered for all the cases according to the IEA data for German transmission lines [100].

4.2 Input Data: Costs

The investment capacity costs are based on annuity and fixed operation and maintenance (O&M) costs, and the marginal costs are based on variable O&M costs, the carrier costs, and the efficiencies. The carbon costs are not considered in the marginal costs since the system is 100% renewable. The required data for calculating the costs, such as capital expenditure, lifetime, the Weighted Average Cost of Capital (WACC), storage capacity cost, carrier cost, fixed and variable O&M costs, efficiencies, and maximum hours for storages, are taken from various references, which are summarized in Table A.1 in Appendix A.

5. Scenarios

Three scenarios, namely *Base*, *Conservative*, and *Progressive*, are developed and analyzed to answer the research questions in different conditions. The volatile generator inputs remain the same in all scenarios. The existing PHS and ACAES capacities also stay the same. The variation of the other parameters for different scenarios is shown in Table 3.

Table 3. Parametric variation for different scenarios

Scenario	Electricity Demand [TWh_{el}]	Total Heat Demand [TWh_{el}]	Total Grid Capacity [GW_{el}]	Biomass Available Potential [PJ]	Electricity Storage Potential* [GW_{el}]	Heat Storage Potential [GW_{th}]
Base	532.77	648.53	35	634.33	Li-ion: 15.65	7.5
					Redox: 0.93	
					ACAES: 1.71	
Conservative	586.04	648.53	32	697.76	Li-ion: 15.65	5
Progressive	479.49	583.68	38	570.89	Li-ion: 15.65	10
					Redox: 0.93	
					ACAES: 3.43	
					H_2: 10.1	

*In addition to these investment potentials, the existing storage capacities of PHS and ACAES are considered for all three scenarios.

5.1 Base Scenario

In the base scenario, it is assumed that electricity and heating demands remain the same as the representative year (2011) in 2050. For storage, Li-ion batteries, PHS, and ACAES (NDE) are considered. The full biomass potential from forest residues, livestock effluents, and agricultural residues in Germany is used as CHP input. For the electrical storage, Li-ion and Redox batteries up to their maximum potentials are used. Besides, half of the total ACAES potential is considered for investment.

5.2 Conservative Scenario

In the conservative scenario, it is assumed that the electricity demand will increase by 10% than the base scenario in 2050. The heating demand is kept the same as the base scenario. For the grid transmission from NDE to SDE, a reduced transfer capacity is considered. To handle the excess electrical demand, an additional

10% biomass import is considered on top of the full potential of Germany. For storage, ACAES and Redox investment possibilities are omitted, and only Li-ion battery investment is considered.

5.3 Progressive Scenario

In the progressive scenario, it is assumed that both the electricity and heat demands (both space and hot water) will reduce by 10% than in the base scenario in 2050. For the grid transmission from NDE to SDE, increased maximum capacity is considered. The maximum usage of biomass is reduced by 10%. All types of electrical (including H_2) and heat storages are optimized for investment up to their full potentials.

6. Results & Discussions

6.1 Sufficiency of the Energy System

All three scenarios reach feasible optimization solutions. Therefore, it is possible to meet the electricity, space heat, and hot water demand in Germany with its renewable resources. However, in the conservative scenario, it is observed that with higher electricity demand and reduced storage and grid capacities, additional biomass import is necessary. Scenario-wise details on the sufficiency of the German energy system to balance supply and demand in both NDE and SDE are discussed below.

6.1.1 Base Scenario

Figure 6 (a) shows the variation of generation and demand in the electricity bus of the NDE energy system for the base scenario in 2050. In NDE, offshore wind can be seen as the dominant resource, providing 188.43 TWh_{el} over the year. Onshore wind is the second-most prevalent resource that supplies a total of 155.19 TWh_{el}. Other resources such as CHP, solar PV, and Hydro ROR plants provide 39.19 TWh_{el}, 17.4 TWh_{el}, and 0.4 $TWh_{el,}$ respectively. Figure 6 (b) shows the percentage-wise use of different electricity generators over the year in the NDE energy system for the base scenario.

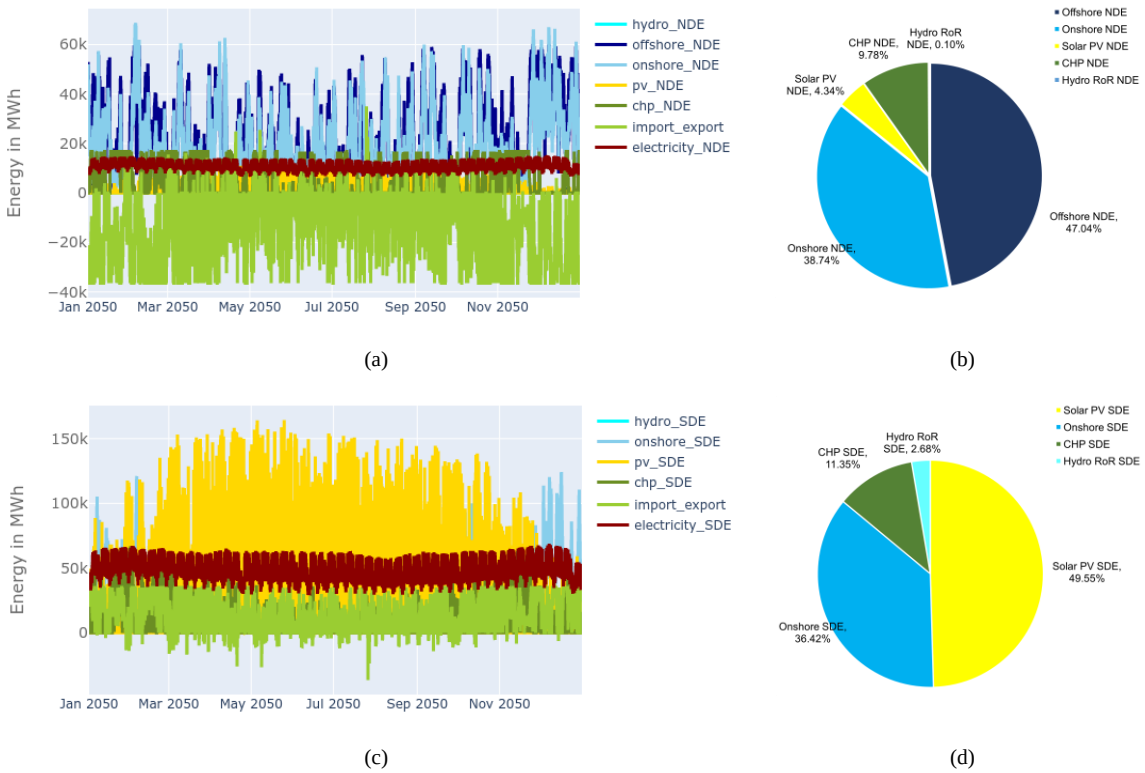

Figure 6: Optimization results of the electricity buses in the base scenario in 2050 (a) supply-demand variation for NDE (b) %-wise use of electricity generators for NDE (c) supply-demand variation for SDE (d) %-wise use of electricity generators for SDE.

Figure 6 (c) shows the variation of generation and demand in the electricity bus of SDE for the base scenario in 2050. In SDE, solar PV is the most dominant resource, supplying 269.38 TWh_{el} over the year. Onshore wind is the second-most prevalent resource delivering a total of 197.98 TWh_{el}. CHP and Hydro ROR plants provide 61.71 TWh_{el} and 14.56 $TWh_{el,}$ respectively. Figure 6 (d) shows the percentage-wise use of different generators in the SDE energy system for electricity generation.

The light green lines in Figure 6 (a) and Figure 6 (c) indicate electrical energy transmission via the NDE-SDE link. The majority of electricity transmission is from NDE to SDE, which shows a total export of 122.22 TWh_{el} from NDE to SDE to supply the electricity shortage in the SDE energy system. On the other hand, the electricity shortage in NDE is much less, since only 3.3 TWh_{el} was delivered from SDE to NDE over the year.

Figure 7 (a) shows the variation of heat supply and demand and the usage of TES in the heat bus of NDE for the base scenario in 2050. GSHP is the most dominant heat supplier, supplying 66.86 TWh_{th} over the year. CHP and ASHP provide the rest of the heat demand, 39.19 TWh_{th} and 16.11 TWh_{th} respectively. The heat storages are used throughout the year up to their exogenously given maximum potential, 1.35 GW_{th}. Figure 7 (b) shows the percentage-wise use of different generators in the NDE energy system for heat generation.

Figure 7: Optimization results of the heat buses in the base scenario in 2050 (a) supply-demand variation for NDE (b) %-wise use of heat generators for NDE (c) supply-demand variation for SDE (d) %-wise use of heat generators for SDE.

Figure 7 (c) shows the variation of supply-demand and heat usage in SDE for the base scenario in 2050. GSHP dominates the other heat generators by a considerable margin, supplying more than 86% (460.7 TWh_{th}) of the total heat generation over the year. CHP provides 61.1 $TWh_{th,}$ and ASHP provides 13.47 TWh_{th} to meet the rest of the demand. The heat storages are used throughout the year up to their maximum potential, 6.15 GW_{th}. Figure 7 (d) shows the percentage-wise use of heat generators in SDE.

Figure 8 (a) shows the usage of electricity storage over the year in NDE for the base scenario. Besides using the full capacities of existing ACAES and PHS plants, the optimization suggests an additional investment of 0.15 GW_{el} of ACAES, 2.82 GW_{el} Li-ion, and 0.17 GW_{el} Redox batteries. Similarly, in SDE, while the existing full capacity of PHS is used for most of the year, an additional investment of 12.83 GW_{el} Li-ion and 0.76 GW_{el} Redox batteries are suggested, as shown in Figure 8 (b). Therefore, in the base scenario, the model suggests full utilization of the exogenously provided maximum capacities for both Li-ion and Redox batteries and partial utilization of the ACAES potential for the German energy system.

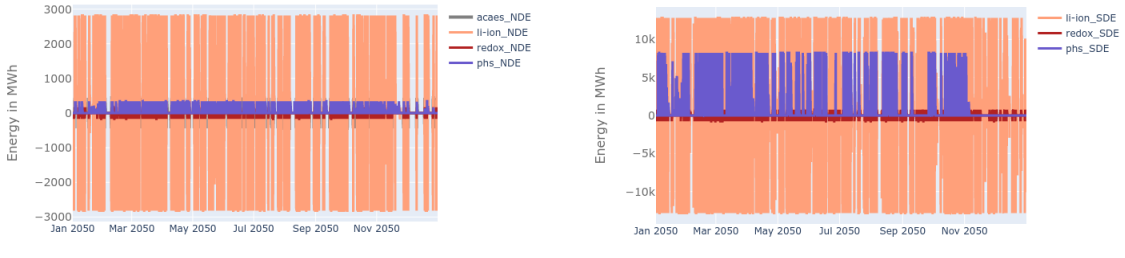

Figure 8: Electricity storage usage in the base scenario in 2050 (a) NDE (b) SDE

6.1.2 Conservative Scenario

Figure 9 (a) shows the variation of generation and demand in the electricity bus of the NDE energy system for the conservative scenario in 2050. Like the base scenario, offshore wind and onshore wind remain the top two electricity resources supplying 257.98 TWh_{el} and 155.19 TWh_{el}. Solar PV, CHP, and hydro ROR plants supply 67.97 TWh_{el}, 43.11 TWh_{el}, and 0.4 TWh_{el}, respectively. Since the electricity demand is increased compared to the base scenario, the excess demand is met by the additional offshore, solar PV, and CHP installations. Figure 9 (b) shows the percentage-wise use of different electricity generators over the year in NDE for the conservative scenario.

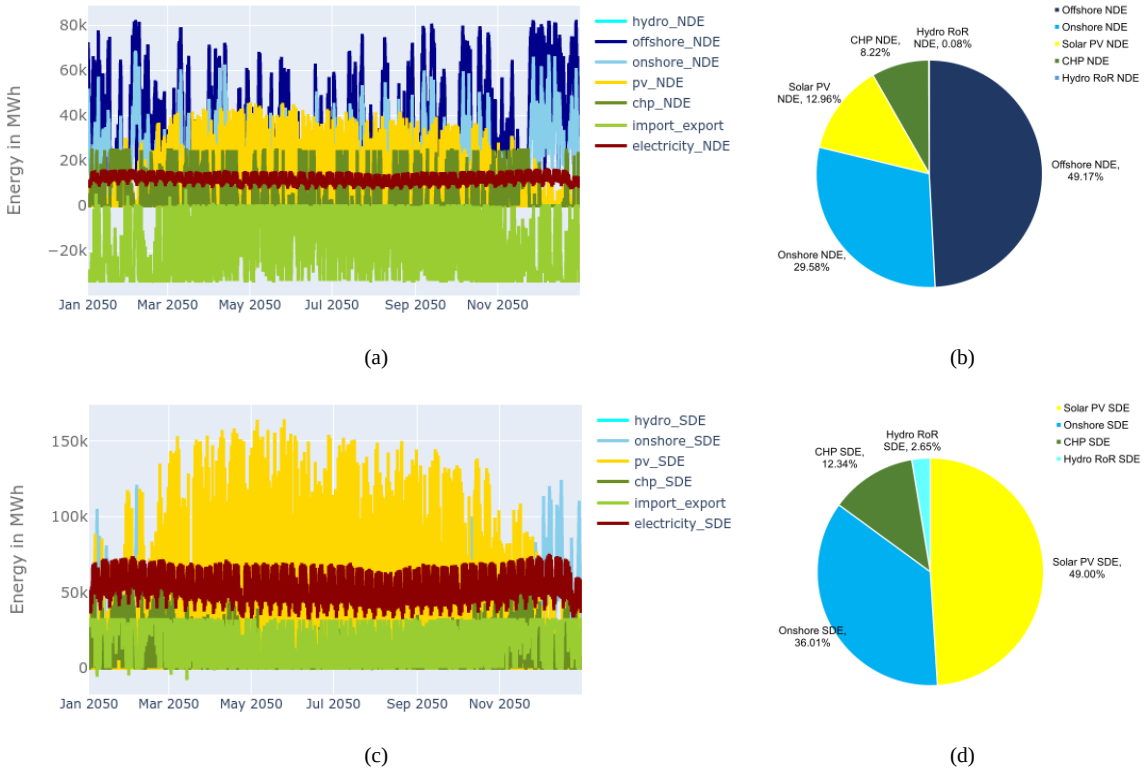

Figure 9: Optimization results of the electricity buses in the conservative scenario in 2050 (a) supply-demand variation for NDE (b) %-wise use of electricity generators for NDE (c) supply-demand variation for SDE (d) %-wise use of electricity generators for SDE.

Figure 9 (c) shows the variation of generation and demand in the electricity bus of the SDE energy system for the conservative scenario in 2050. While solar PV, onshore wind, and hydro ROR plants provide the same amount of energy as in the base scenario, the excess electricity demand is met by installing additional CHP plants, providing 67.83 TWh_{el} over the year. Figure 9 (d) shows the percentage-wise use of different electricity generators over the year in the SDE energy system for the conservative scenario.

In SDE, onshore, solar PV, and hydro ROR capacities are already installed to their maximum capacities in both base and conservative scenarios. Therefore, the excess demand in SDE can be met by the additional biomass-based CHP, offshore, and solar PV facilities in NDE. Consequently, an increase in the electricity export totaling 143.16 TWh_{el} over a year from NDE to SDE is observed. On the contrary, the export from SDE to NDE reduces to a total of 0.04 TWh_{el} since there are more offshore and PV installations in NDE in the conservative scenario than in the base scenario.

Figure 10 (a) shows the variation of heat supply and demand and the usage of TES in the heat bus of NDE for the conservative scenario in 2050. The heat generator order remains the same as the base scenario in the conservative scenario, where GSHP, CHP, and ASHP supply 65.04 TWh_{th}, 43.11 TWh_{th}, and 18.5 TWh_{th}, respectively. The heat storages are used up to their reduced maximum potential of 0.9 GW_{th}. Figure 10 (b) shows the percentage-wise use of different heat generators for the conservative scenario in NDE.

Figure 10: Optimization results of the heat buses in the conservative scenario in 2050 (a) supply-demand variation for NDE (b) %-wise use of heat generators for NDE (c) supply-demand variation for SDE (d) %-wise use of heat generators for SDE.

Figure 10 (c) shows the heat supply-demand variation and TES usage in the heat bus of SDE for the conservative scenario in 2050. The heat generator order remains the same as the base scenario, where GSHP, CHP, and ASHP supply a yearly total of 457.73 TWh_{th}, 67.7 $TWh_{th,}$ and 8.2 $TWh_{th,}$ respectively. The heat storages are used throughout the year to their reduced maximum potential, i.e., 4.1 GW_{th}. Figure 10 (d) shows the percentage-wise use of different heat generators for the conservative scenario in SDE.

In the conservative scenario, besides the existing PHS and ACAES capacities, only Li-ion battery investment is considered. Figure 11 (a) shows the usage of electricity storages over the year in NDE for the conservative scenario, where the optimization suggests an additional investment of the full available capacity of Li-ion batteries (i.e., 2.81 GWel). Figure 11 (b) shows a similar pattern for SDE, where the model suggests an additional investment of 12.83 GW_{el} Li-ion batteries.

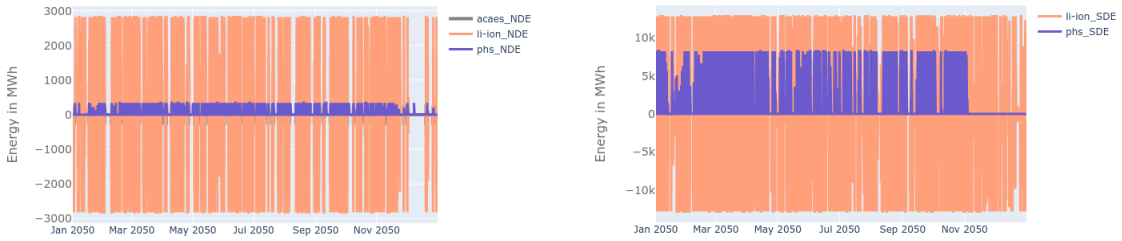

Figure 11: Electricity storage usage in the conservative scenario in 2050 (a) NDE (b) SDE

6.1.3 Progressive Scenario

Figure 12 (a) shows the supply-demand variation in the electricity bus of NDE for the progressive scenario in 2050. With reduced heat and electricity demand and fewer offshore installations, onshore wind becomes the most dominant electricity supplier in this scenario, providing 155.19 TWh_{el} over the year. Energy generation from offshore wind, CHP, and solar PV plants decrease in this scenario, with a total supply of 101.17 TWh_{el}, 35.27 TWh_{el}, and 8.11 $TWh_{el,}$ respectively. Hydro ROR supply remains the same (i.e., 0.4 TWh_{el}) in all three scenarios. Figure 12 (b) shows the percentage-wise use of the electricity generators for the progressive scenario in NDE.

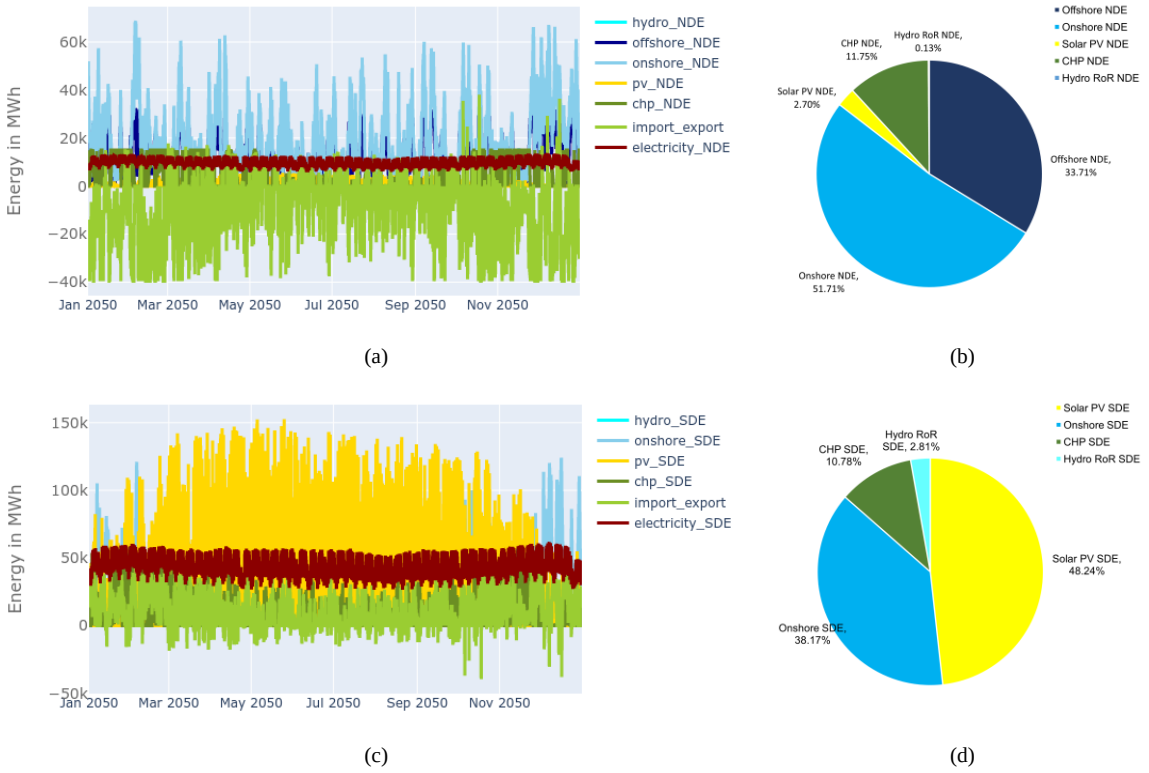

Figure 12: Optimization results of the electricity buses in the progressive scenario in 2050 (a) supply-demand variation for NDE (b) %-wise use of electricity generators for NDE (c) supply-demand variation for SDE (d) %-wise use of electricity generators for SDE.

Figure 12 (c) shows the supply-demand variation in the electricity bus of SDE for the progressive scenario in 2050. The total energy supplying merit order remains the same, with solar PV being the most dominant resource, followed by onshore wind, CHP, and hydro ROR plants, supplying 250.22 TWh_{el}, 197.98 TWh_{el}, 55.92 $TWh_{el,}$ and 14.56 TWh_{el} respectively. While onshore wind and hydro ROR supply remain the same, supply from solar PV and CHP is reduced than the other two scenarios because of the reduced electricity and heat demand. Figure 12 (d) shows the percentage-wise use of the electricity generators in SDE.

With reduced electricity and heat demand but further storage options, electricity export from NDE to SDE is much reduced than the previous two scenarios, totaling 94.56 TWh_{el} over the year. On the other hand, comparatively less offshore wind, CHP, and solar PV installations in NDE expanded NDE-SDE grid connection, and additional storage flexibility in both NDE and SDE helps to balance the demand of the NDE with more power from the south. Therefore, in the progressive scenario, a total of 6.26 TWh_{el} is transferred from SDE to NDE, which is higher than both base and conservative scenarios.

Figure 13 (a) shows the variation of heat supply and demand and the usage of TES in the heat bus of NDE for the progressive scenario in 2050. With the same merit order of the other two scenarios, GSHP, CHP, and ASHP produce 58.74 TWh_{th}, 35.27 $TWh_{th,}$ and 13.2 TWh_{th} throughout the year. The heat storages are used throughout the year up to their maximum potential of 1.8 GW_{th}. Figure 13 (b) shows the percentage-wise use of different heat generators for the progressive scenario in NDE.

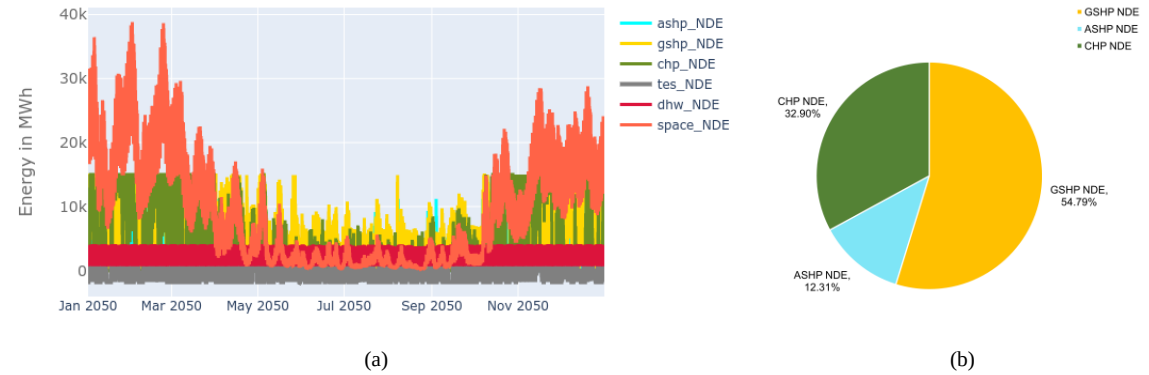

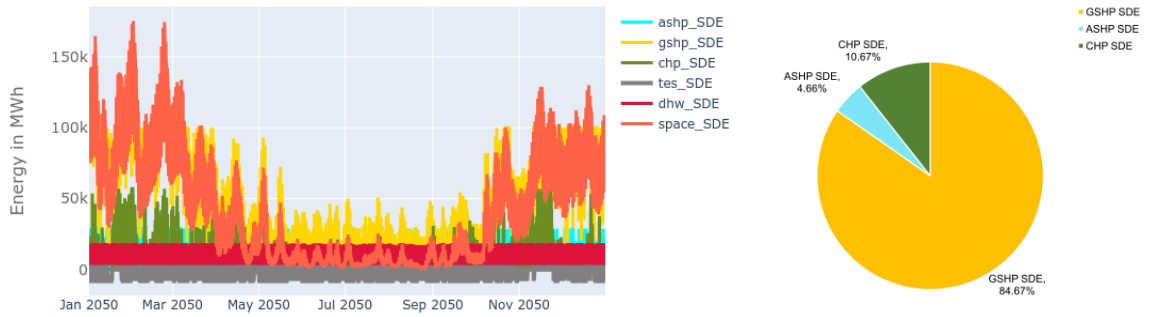

(c) (d)

Figure 13: Optimization results of the heat buses in the progressive scenario in 2050 (a) supply-demand variation for NDE (b) %-wise use of heat generators for NDE (c) supply-demand variation for SDE (d) %-wise use of heat generators for SDE.

Figure 13 (c) shows the supply-demand variation and TES usage in the heat bus of SDE for the progressive scenario in 2050. The merit order remains the same as the other two scenarios where GSHP, CHP, and ASHP provide 409.28 TWh_{th}, 51.6 $TWh_{th,}$ and 22.53 $TWh_{th,}$ respectively. The heat storages are used up to their increased maximum potential of 8.2 GW_{th}. Figure 13 (d) shows the percentage-wise use of different heat generators for the progressive scenario in SDE.

Figure 14 shows the usage of electricity storage over the year in NDE and SDE for the progressive scenario. In addition to the investment in batteries up to their max potentials (i.e., 15.65 GW_{el} investment for Li-ion and 0.93 GW_{el} investment for Redox), the model suggests an additional investment of 0.51 GW_{el} in ACAES. Although Hydrogen storage is one of the inputs of this scenario, the optimization does not suggest the installation of H_2 storage in any of the energy systems.

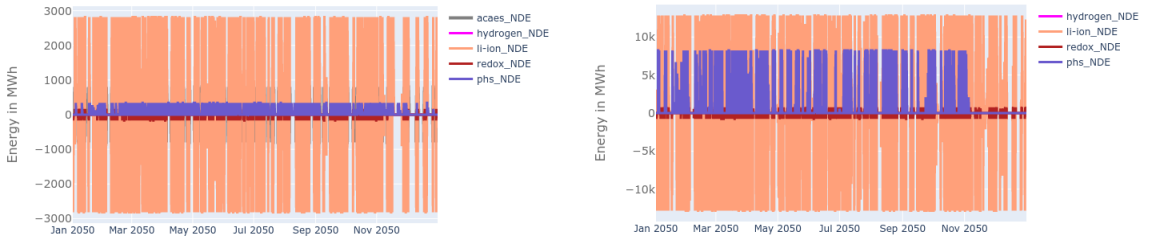

(a) (b)

Figure 14: Electricity storage usage in the progressive scenario in 2050 (a) NDE (b) SDE

6.2 Capacities and Investments

6.2.1 Volatile Generator

6.2.1.1 Volatile Generator Capacity and Investment

Figure 15 compares the existing capacities and required investments of the volatile generators for all three scenarios. While the different colors show the capacities and investments for NDE and SDE, each column represents a scenario considering both installed capacity and required investment in the whole of Germany. For onshore wind plants illustrated by Figure 15 (a), in addition to the existing 53.91 GW_{el}, investment in 168.69 GW_{el} (i.e., the maximum onshore wind potential) is necessary for all three scenarios for Germany, of which 49.88 GW_{el} is in the NDE, and 118.81 GW_{el} is in the SDE energy system. Therefore, the model suggests maximum utilization of the available potential of all onshore wind energy in Germany. In the case of offshore wind plants shown by Figure 15 (b), on top of the existing 6.66 GW_{el}, the base scenario suggests installing 54.4 GW_{el}, the conservative scenario recommends installing 76.94 GW_{el} (i.e., the maximum offshore wind potential), and the progressive scenario suggests installing 26.13 GW_{el} capacities.

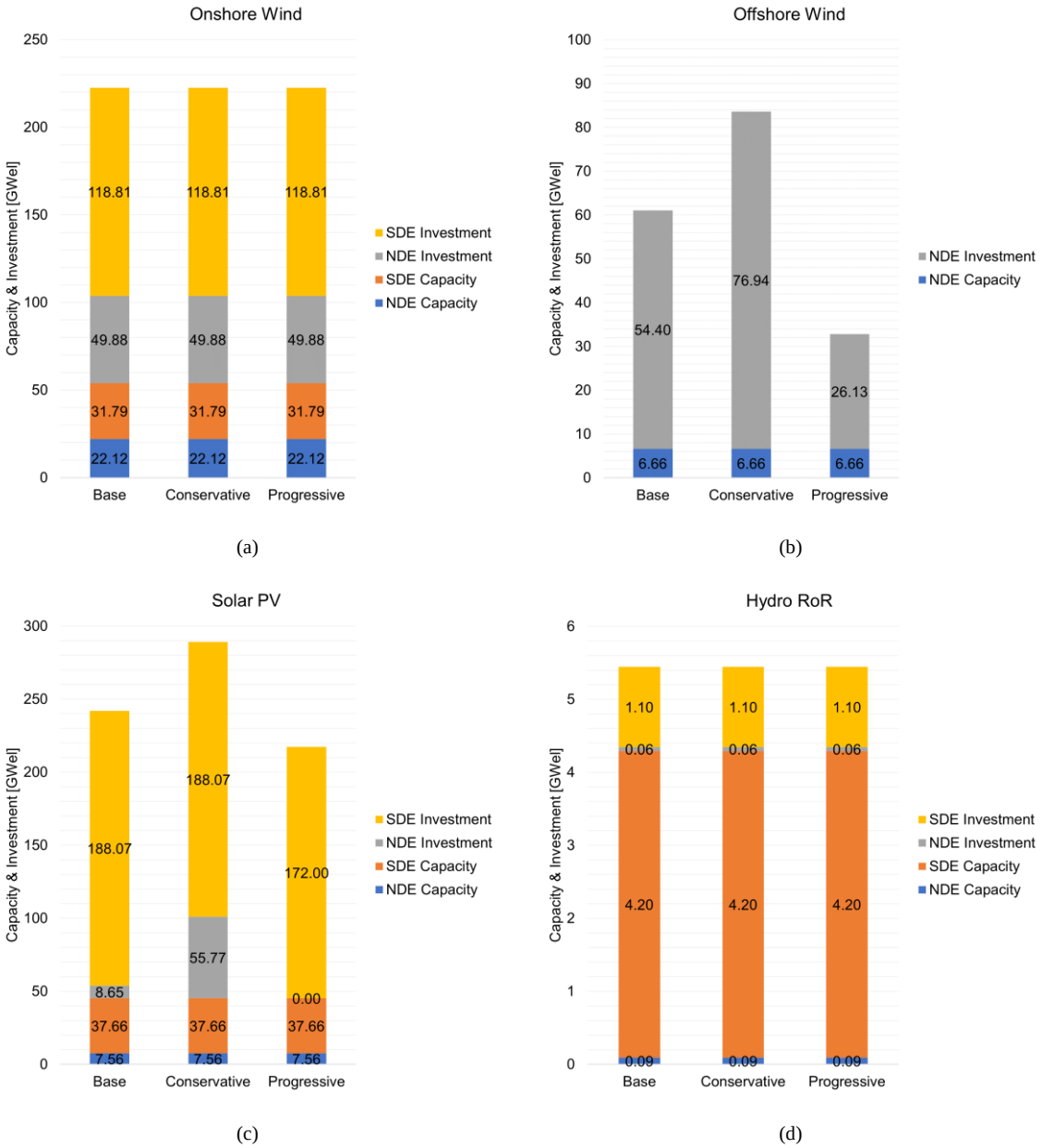

Figure 15: Scenario-wise comparison of installed capacity and required investments for volatile generators in Germany (a) onshore wind (b) offshore wind (c) PV (d) hydro ROR plants.

For solar PV, as shown in Figure 15 (c), in addition to the existing 45.23 GW_{el} capacity, the base and conservative scenarios suggest utilizing the full solar potential of Southern Germany, i.e., 188.07 GW_{el} in the SDE energy system. Contrarily, the progressive scenario in SDE suggests a reduced solar PV installation of 172 GW_{el}. In Northern Germany, where solar PV potential is comparatively less, the model suggests installing 8.65 GW_{el} in the base scenario and 55.77 GW_{el} in the conservative scenario (maximum solar PV potential). Interestingly, the progressive scenario suggests that no additional solar PV installation is necessary for NDE. In the case of Hydro ROR plants shown by Figure 15 (d), both the NDE and SDE systems for all three scenarios suggest capacity increment up to the maximum available potentials, i.e., 0.06 GW_{el} in NDE and 1.1 GW_{el} in SDE, on top of the existing 4.29 GW_{el} in Germany.

6.2.1.2 Volatile Generator Investment Cost

Figure 16 shows the technology-wise investment costs of the volatile generators for NDE and SDE and the total costs for each of the scenarios in Germany. As shown in Figure 16 (a), the annual investment cost remains the same in all three scenarios for onshore wind plants (9.84 bn €/yr) and hydro ROR plants (0.19 bn €/yr). For offshore wind, the annual investment is 7.92 bn €/yr, which increases in the conservative scenario (11.2 bn €/yr) and decreases in the progressive scenario (3.8 bn €/yr). Similarly, in solar PV, the base scenario investment of 4.33 bn €/ yr goes high in the conservative scenario (5.37 bn €/yr) and goes low in the progressive scenario

(3.79 bn €/yr). Figure 16 (b) compares the total investment cost for all volatile generators in the German energy system for different scenarios. The annual investment cost for all the volatile generators is 22.28 bn €/yr, which increases by more than 19% in the conservative scenario (26.6 bn €/yr) and decreases by around 21% in progressive scenario (17.62 bn €/yr).

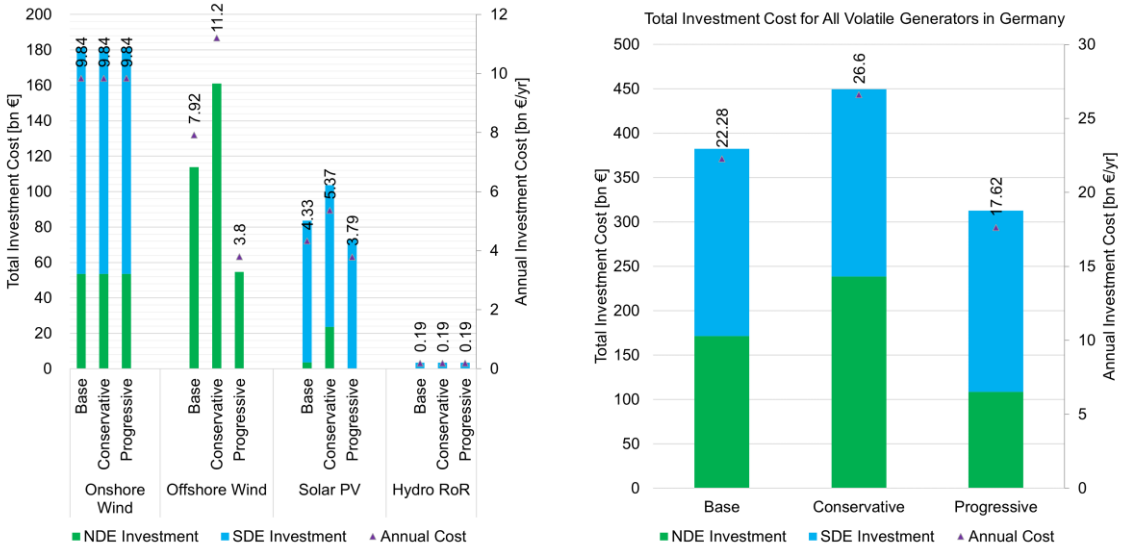

(a) (b)

Figure 16: Scenario-wise comparison of investment costs for volatile generators in Germany (a) technology-wise comparison (b) total investment cost for all volatile generators. The primary vertical axis (left) shows the total investment cost for the whole time-horizon in billion euros (shown as stacked columns), and the secondary vertical axis (right) shows the annual investment cost in billion euros/year (shown in markers).

6.2.2 CHP and Heat Pump

6.2.2.1 CHP and Heat Pump Capacity and Investment

Figure 17 compares the existing capacities (only CHP) and required investments for the heat generators for each scenario. For CHP shown by Figure 17 (a), in addition to the existing 13.6 GW, investment in 68.61 GW, 73.62 GW, and 58.26 GW, additional capacities are necessary for the base, conservative, and progressive scenarios, respectively. Figure 17 (b) shows a similar pattern for heat pumps (combining GSHP and ASHP) in Figure 17 (b), where the base scenario requires 173.41 GW_{th} investment, the conservative scenario requires an increased 181.86 GW_{th} investment, and the progressive scenario requires a decreased 154.93 GW_{th} investment in Germany.

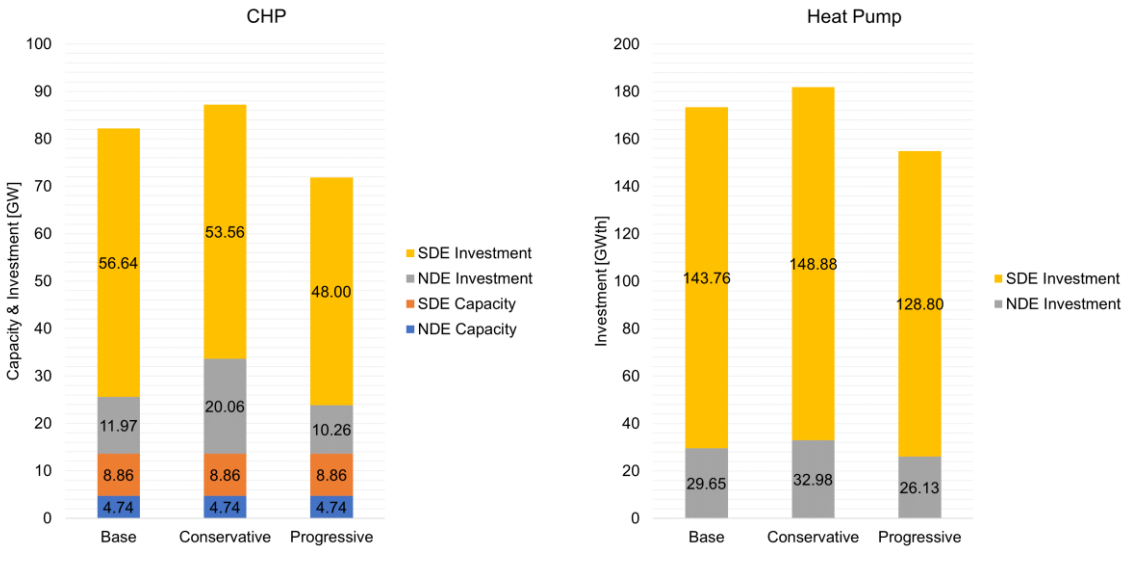

(a) (b)

Figure 17: Scenario-wise comparison of installed capacity and required investments for CHP and Heat Pump in Germany (a) CHP (b) Heat Pump (GSHP and ASHP).

Although the heat demand did not change in the conservative scenario, heat generator installations increases because of the following reasons:

1. Since volatile generators are already installed up to their maximum potential, increased CHP installations are required to meet the additional electricity demand;
2. Reduced grid transfer capacity minimizes the scope for power exchange between the grids and hence lessen the scope of P2H conversion with power from the other energy system. This circumstance enforces the model to install additional local heat pumps in individual energy systems;
3. Heat generation in this energy system is dependent upon both electrical (because of P2H) and heat storage. Since both electrical and heat storages are reduced in the conservative scenario, supply-demand balancing requires additional heat generators.

This additional heat generator in the conservative scenario also results in surplus heat in both energy systems at different hours over the year. Nevertheless, this problem of additional heat investment is minimized in the progressive scenario where we have reduced electricity and heat demands, increased grid transfer capacity, and increased electrical and heat storage. Therefore, the investment in both CHPs and heat pumps are lowered in the progressive scenario, as shown in Figure 17.

6.2.2.2 CHP and Heat Pump Investment Cost

Figure 18 shows the technology-wise investment costs of the CHPs and heat pumps for NDE and SDE and the total costs for each of the scenarios in Germany. As shown in Figure 18 (a), the annual investment cost for CHPs in the base scenario is 8.71 bn €/yr, which increases to 9.34 bn €/yr in the conservative scenario, and decreases to 7.39 bn €/yr in the base scenario. Similarly, for heat pumps, the base scenario investment of 18.47 bn €/yr increases to 19.44 bn €/yr in the conservative scenario, and decreases to 16.28 bn €/ yr in the progressive scenario. Figure 18 (b) compares the total investment cost for all CHPs and heat pumps in the German energy system for different scenarios. The annual investment cost for all the heat generators is 27.18 bn €/yr, which increases by more than 5% in the conservative scenario (28.78 bn €/yr), and decreases by around 13% in the progressive scenario (23.67 bn €/yr).

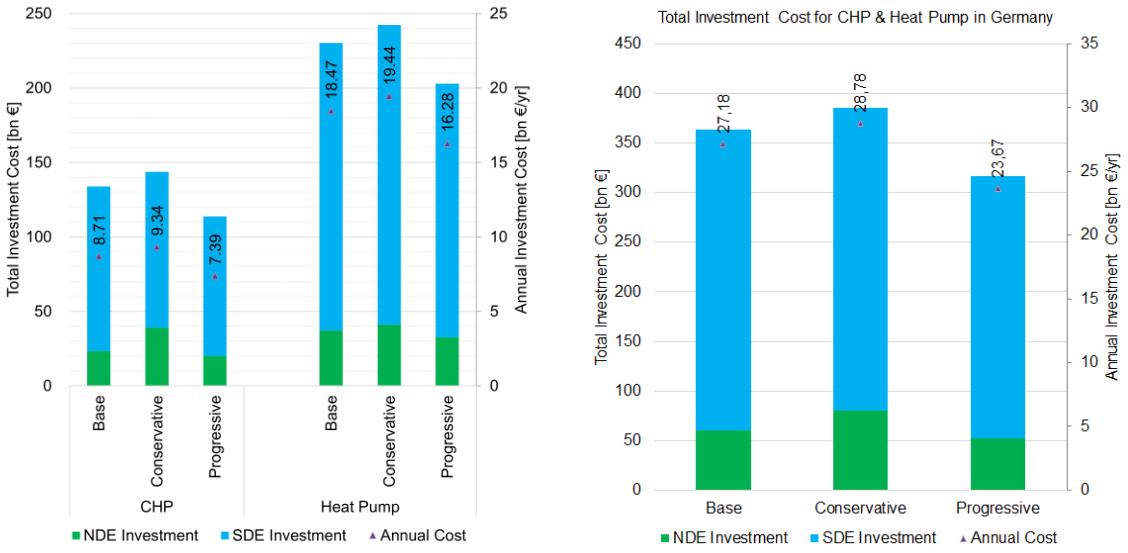

(a) (b)

Figure 18: Scenario-wise comparison of investment costs for CHP and heat pump in Germany (a) technology-wise comparison (b) total investment cost for all heat generators (CHPs & heat pumps). The primary vertical axis (left) shows the total investment cost for the whole time-horizon in billion euros (shown as stacked columns), and the secondary vertical axis (right) shows the annual investment cost in billion euros/year (shown in markers).

6.2.3 Storage

6.2.3.1 Storage Capacity and Investment

Figure 19 compares the investment for all types of storage. Although the scenarios had H_2 as an input, the model does not suggest any investment in H_2 storage. Figure 19 (a) and Figure 19 (b) shows the required investment capacities of Li-ion and Redox batteries. Both batteries are used up to their maximum given potential, whenever used as an input. According to Figure 19 (a), for a total of 15.65 GW_{el} Li-ion batteries, the total optimized energy capacity is 102 GWh_{el} (NDE=18.32 GWh_{el}, SDE=83.42 GWh_{el}). As shown in Figure 19

(b), for 0.93 GW_{el} Redox batteries in Germany, the total optimized energy capacity is 3 GWh_{el} (NDE= 0.56 GWh_{el}, SDE=2.52 GWh_{el}). However, the ACAES are used partially with an optimized power of 0.15 GW_{el} and optimized energy storage of 2.5 GWh_{el} in the base scenario, and an increased optimized capacity of 0.51 GW_{el} and optimized energy storage of 5 GWh_{el} in the progressive scenario, as shown in Figure 19 (c). Figure 19 (d) shows the usage of TES capacities up to their maximum exogenous potential, with the total optimized energy storage capacity varying in between 360 GWh_{th} (conservative) and 720 GWh_{th} (progressive).

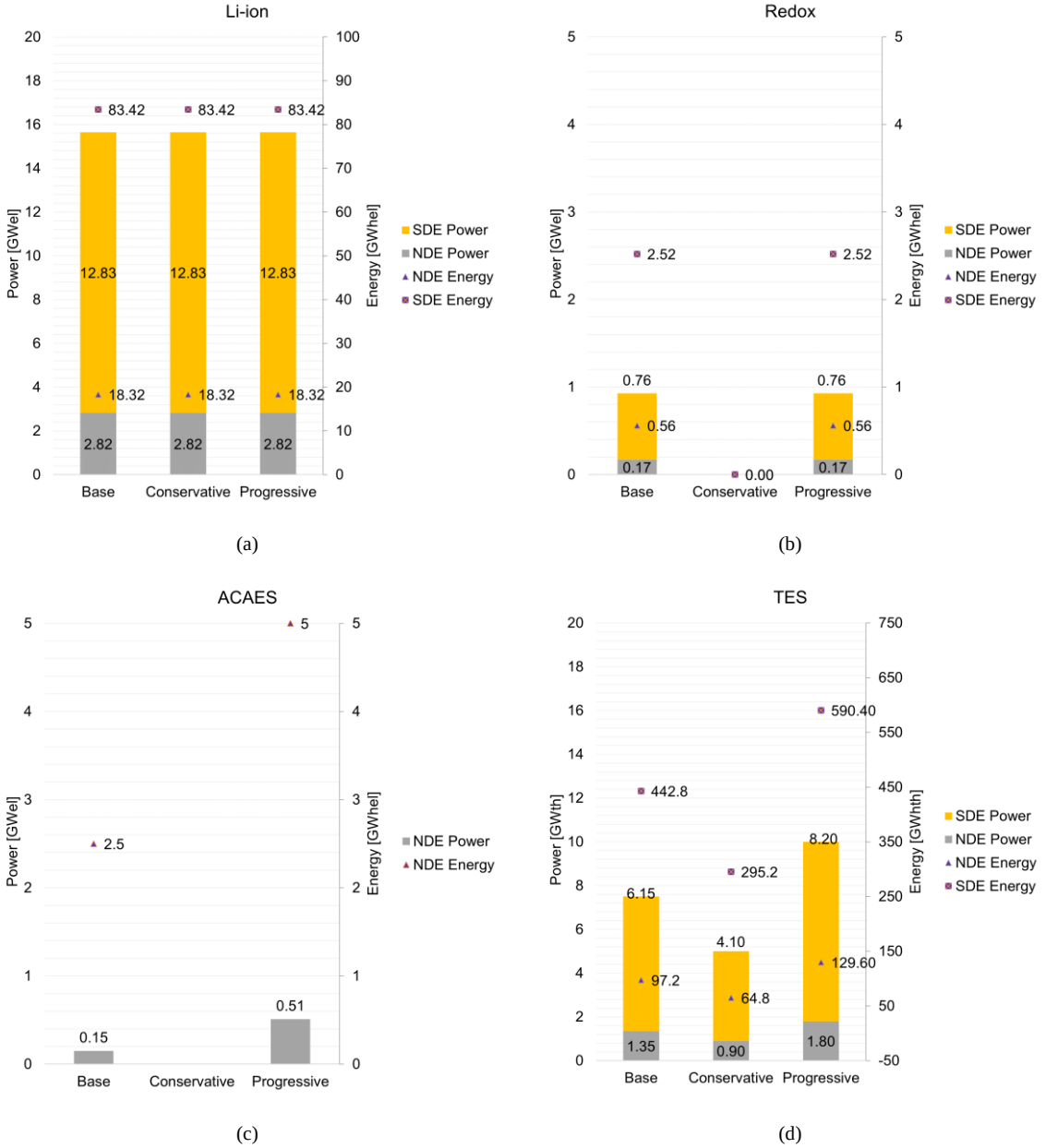

Figure 19: Scenario-wise comparison of required power and energy storage investments for electrical and heat storages in Germany (a) Li-ion (b) Redox (c) ACAES (d) TES. The primary vertical axis (left) shows the power capacity in GW_{el}/GW_{th} (shown as stacked columns), and the secondary vertical axis (right) shows the energy storage capacity GWh_{el}/GWh_{th} (shown in markers).

6.2.3.2 Storage Investment Cost

Figure 20 shows the investment costs of the electrical and heat storage for NDE and SDE, and the total costs for each of the scenarios in Germany. As shown in Figure 20 (a), the annual investment cost for Li-ion batteries in all three scenarios is 1.57 bn €/yr. For Redox batteries, the annual investment cost in the base scenario and the progressive scenario is 0.05 bn €/yr. In the case of ACAES, the annual investment cost is 0.01 bn €/yr in the base scenario, and 0.03 bn €/yr in the progressive scenario. The annual investment cost of heat storage depends mainly upon the volume of the storage capacity, which is 1.66 bn €/yr in the base scenario for 540 GWh_{th}. As the storage capacity goes down to 360 GWh_{th} in the conservative scenario, the yearly investment reduces to 1.1 bn €/yr. In the progressive scenario, the annual investment again increases to 2.21 bn €/yr, since the total storage capacity of Germany increases to 720 GWh_{th}. Figure 20 (b) shows the total investment costs

for all storages in Germany according to the model results. The annual investment for all storages is 3.29 bn €/yr in the base scenario, which decreases by more than 18% to 2.67 bn €/yr in the conservative scenario with reduced storage provisions, and increases by around 17% to 3.86 bn €/yr in the progressive scenario with high storage provisions.

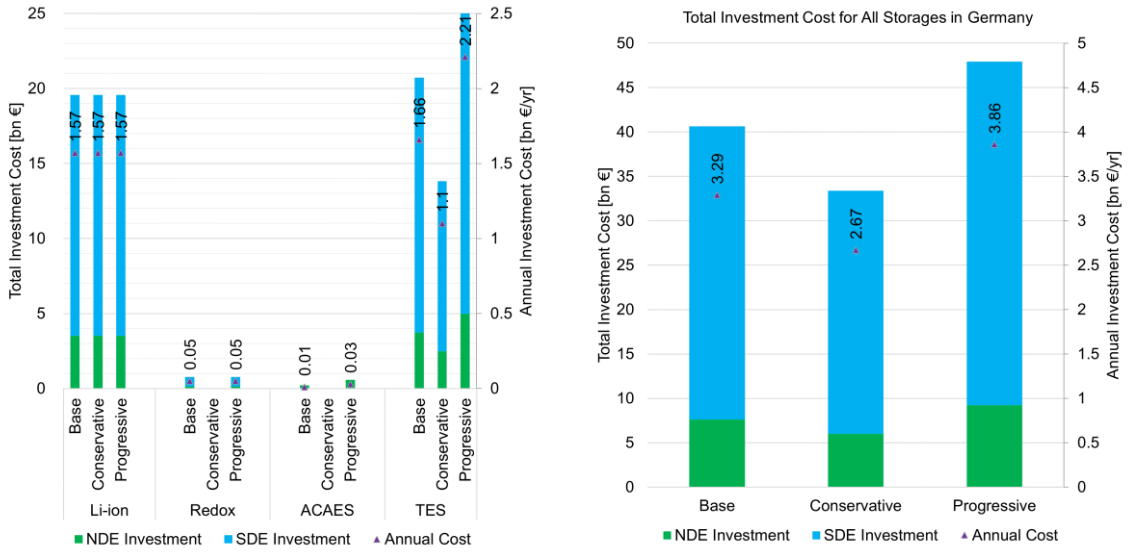

(a) (b)

Figure 20: Scenario-wise comparison of investment costs for electrical and heat storages in Germany (a) technology-wise comparison (b) total investment cost for all storages. The primary vertical axis (left) shows the total investment cost for the whole time-horizon in billion euros (shown as stacked columns), and the secondary vertical axis (right) shows the annual investment cost in billion euros/year (shown in markers).

6.3 Energy Mix and Flexibility Aspects

6.3.1 Energy Mix

Figure 21 compares the energy mix results from different scenarios. Figure 21 (a) shows the composition of the electricity generation mix. The total electricity generation in the base scenario is 944 TWh_{el}, which can increase to 1074 TWh_{el} in the conservative scenario with excess demand, less storage, and reduced grid capacity; and decrease to 818 TWh_{el} in the progressive scenario with reduced demand, more storage, and increased grid capacity. The energy mix also shows that, while all three scenarios need maximum offshore wind and hydro ROR, additional solar PV, offshore wind, and CHP supply the rest of the demand. The base scenario mix comprises 37% onshore wind, 19% offshore wind, 30% solar PV, 10% CHP, and 0.01% hydro ROR plants. The progressive scenario shows similar results: 43% onshore wind, 12% offshore wind, 31% solar PV, 11% CHP, and 0.01% hydro ROR. These two results can be compared with the study by Fraunhofer Institute, where they concluded that in an 85% system, the electricity generation is close to 800 TWh_{el}, of which onshore wind is 47%, offshore wind is 16%, and solar PV is 22% [101]. Therefore, the results from the OSEeM-DE model suggest that a transformation towards 100%-system is feasible by 2050, and the energy mix (in merit order) consists of onshore wind, solar PV, offshore wind, CHP, and hydro ROR plants. CHPs can replace the remaining 15% fossil-fuel-based generation of the 85% system in the Fraunhofer study using the available biomass potential in Germany without importing from other countries. Such a system can also co-exist with a heat sector integrated model incorporating P2H technologies such as heat pumps. It is evident from Figure 21 (b), which compares the heat generation mixes from different scenarios. The heat generation is 657 TWh_{th} in the base scenario, and 660 TWh_{th} in the conservative scenario. Although the heat demand remained the same in both scenarios, the latter shows a higher generation because of less heat storage provision and reduced transfer capacity between systems. However, with less demand, more heat storage capacity, and more grid transfer capacity, the progressive scenario yields a reduced heat generation of 590 TWh_{th}.

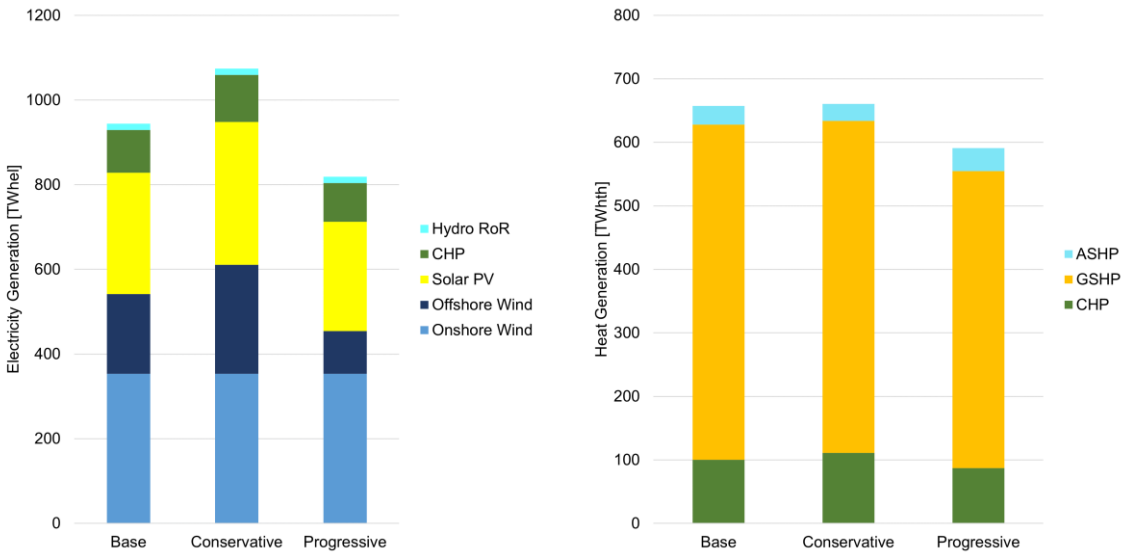

(a) (b)

Figure 21: Scenario-wise comparison for energy generation (a) electricity generation (b) heat generation

The heat generation in all three scenarios also shows that heat pumps dominate the heat generation (around 80%), and biomass-CHPs cover the rest of the demand. In heat pumps, the comparatively more efficient GSHPs are preferable over comparatively less expensive ASHPs. Though the model considers only CHPs and heat pumps, other renewable applications such as electric boiler, solar heating, biofuel heating, hydrogen heating, geothermal heating should be investigated for producing heat, primarily process heating in industries.

Excess generation from renewables is a challenge that needs to be solved using a combination of plausible solutions. The OSeEM-DE results show that the least amount of excess generation occurs in the progressive scenario, indicating the apparent solution of using more storages. Also, the developed model is currently an island model with no interconnection between neighboring countries. A German energy system and its neighboring countries can reduce the curtailment problem with reduced optimized generation and storage capacities. Furthermore, demand response activities and the inclusion of the transport sector with electric vehicles are also needed to reduce the curtailment or utilize the excess generation.

The Levelized cost of electricity (LCOE) is calculated from the optimization results according to (23) (See Section 3.9). These LCOE values are close to another study report from Fraunhofer ISE, which illustrated a range of learning curve-based predictions of LCOEs in Germany through 2035 [102]. Table 4 compares the LCOE values according to the OSeEM-DE model results and the Fraunhofer ISE's study. The comparison shows that the scenario results for onshore and offshore wind and solar PV technology from OSeEM-DE are within the range predicted in the Fraunhofer ISE report for the year 2035; however, for biomass, the OSeEM-DE results indicate higher LCOE values, resulting from the high fuel cost of biomass.

Table 4: LCOE comparison of Fraunhofer ISE study report values and OSeEM-DE model results

Technology	**Levelized Cost of Electricity [€ cent/kWh]**	
	Fraunhofer ISE Study (2035) [102]	**OSeEM-DE Model (2050)**
Onshore Wind	3.49 - 7.09	4.99
Offshore Wind	5.67 - 10.07	6.34 - 6.93
Solar PV	2.41 - 4.70	3.56 - 3.73
Biomass/Biogas	10.14 - 14.74 (Biogas)	19.47 - 20.26 (Biomass)

6.3.2 Flexibility Aspects

6.3.2.1 Grid Expansion

The primary assumption for this study is the growth of grid connection in 2050, resulting in a significant increase of power exchange between northern and southern Germany. The results from the model for all three scenarios suggest a large amount of grid exchange, especially from NDE to SDE. For example, in the base scenario, around 28% of the SDE electrical demand comes from NDE (122.22 TWh_{el} vs. 436.16 TWh_{el}). Similarly, in the conservative scenario, around 29% of the SDE electrical demand comes from NDE (143.17 TWh_{el} vs. 479.78 TWh_{el}), and in the progressive scenario, around 24% of the SDE demand comes from NDE (94.57 TWh_{el} vs. 392.55 TWh_{el}).

A sensitivity analysis is conducted to inspect the effect of grid expansion on power and heat generator investments, energy transfer, storage. For this analysis, the base scenario is modified where all the storage capacities (including ACAES) are optimizable up to their maximum potentials, and the grid capacity (i.e., the NDE-SDE link) varies in between 25 GW_{el} and 40 GW_{el}. As shown in Figure 22 (a), with the grid expansion from 25 GW_{el} to 40 GW_{el}, the offshore wind investment is reduced by 15% from 59.75 GW_{el} to 50.68 GW_{el}, and the solar PV is reduced by 22% from 241.22 GW_{el} to 188.07 GW_{el}. The onshore wind and hydro ROR investment remain the same. Similarly, the requirement of heat pump installation also decreases by 5% (171.37 GW_{th} vs. 171.21 GW_{th}). However, while increasing grid expansion results in decreasing capacities of offshore wind plants, relatively less expensive biomass-based CHPs replace a share of the curtailed offshore generation. Therefore, CHP installation increases by 2% (66.97 GW vs. 68.30 GW) with the grid expansion from 25 GW_{el} to 40 GW_{el}. Figure 22 (b) shows the increase in the total amount of electricity transfer from between NDE and SDE for increasing grid capacities. For the grid expansion from 25 GW_{el} to 40 GW_{el}, an increase of 2.5% (119.64 TWh_{el} vs. 122.72 TWh_{el}) from NDE to SDE is observed. On the other hand, from SDE to NDE, though the transfer amount is much less in comparison with NDE to SDE, a sharp increment rate can be observed (0.21 TWh_{el} vs. 6 TWh_{el}) when the grid capacity expands.

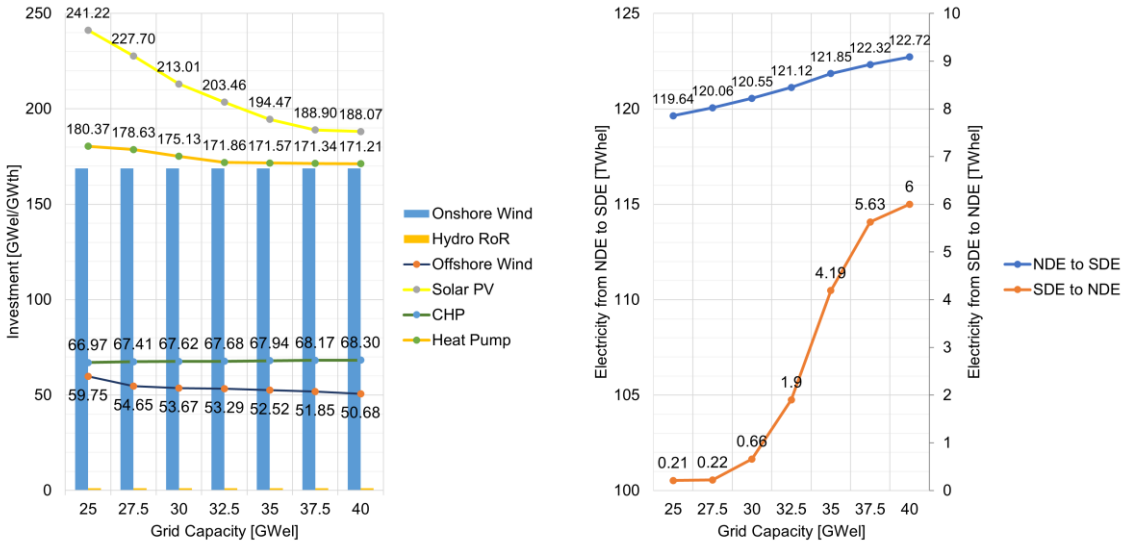

(a) (b)

Figure 22: Effect of grid capacity expansion between Northern and Southern Germany (a) investment in electricity and heat generators. The varying values of offshore wind, solar PV, CHP, and heat pumps are shown using lines, and the steady onshore wind and hydro ROR capacities are shown using columns (b) total annual electrical energy transfer between NDE and SDE. Two different vertical axes are used for showing the exchange, the primary vertical one (left) for NDE to SDE, and the secondary vertical one (right) for SDE to NDE.

Regarding storage, the results for power and energy capacities for all the storage remained constant for all grid capacities, which indicated the maximum usage of the exogenously provided potentials. Therefore, the impact on the storage capacities for the expansion of the grid could not be measured using this sensitivity analysis. However, it is evident that the grid expansion facilitates a smoother balance between the two systems resulting through an increased electricity exchange, thus requiring overall less investment offshore wind, solar PV, and heat pump installations. Therefore, the expansion of the electrical grid between Northern and Southern Germany should be considered as a promising option for supporting a 100% renewable-based sector-coupled system for Germany. However, the cost of grid expansion vs. investment in generation facilities, which has not been conducted in this research, must be investigated to reach an optimum solution and draw a conclusion.

6.3.2.2 Storage and Dispatchable Load

Electrical storages and dispatchable loads (i.e., heat pumps) with heat storage show a tendency towards flexibility and interdependence in all of the scenarios. The existing hydro ROR plants and PHS help the system to balance both the short-term and long-term. Also, the biomass-fed CHPs are used as dispatchable generation resources where the biomass resources serve as a backup to counter the variability of the volatile generation from solar PV and wind. Both Li-ion and Redox batteries act as critical storage technologies to be utilized for shorter periods. On the other hand, ACAES shows promising prospects to aid the PHS for long-term seasonal storage.

The large-scale investment of both GSHP and ASHP from the optimization results confirms the findings of Hedegaard and Münster, i.e., the individual heat pumps can have a positive contribution towards large scale wind power investments to reduce the system cost and pressure on the limited biomass potential [103]. The dispatchable heat pumps can use the surplus power from the variable renewable generation, which supplements the other heat generation sources (in this case, CHP) and offers flexible operations.

A sensitivity analysis is conducted to inspect the effect of storage variation on electrical and heat generators. For this analysis, another modified version of the base scenario is chosen, where the grid capacity (i.e., the NDE-SDE Link) is fixed at 20 GW_{el}, and the batteries (Li-ion and Redox), H_2 storage, and TES are gradually doubled from their current maximum exogenous potential. The ACAES and PHS capacities are not expanded since spatial constraints limit their maximum potentials. As shown in Figure 23 (a), with the increase in storage capacities, the onshore wind, solar PV, and hydro ROR capacities do not change, but the offshore investment drops by more than 47% (55.53 GW_{el} vs. 29.1 GW_{el}) when the storages are doubled. Similarly, both CHP and heat pump investment decreased by more than 13% (62.5 GW vs. 54.32 GW) and 6% (189.87 GW_{th} vs. 177.39 GW_{th}), respectively. Hence, increased storage options offer additional flexibility to curtail peak/reserve capacities for the energy system.

On the other hand, electricity exchange decreases from NDE to SDE by more than 9% (113.88 GW_{el} vs. 102.77 GW_{el}) when the storage capacity is doubled, as shown in Figure 23 (b). Contrarily, the electricity transmission from SDE to NDE is almost a straight line, with a much lower value. The decrease of investment in offshore wind, CHP, and heat pumps and the reduced energy transfer from NDE to SDE indicate that storage expansion in local energy systems can be another viable flexibility option for reducing investment in generation capacities and grid expansion.

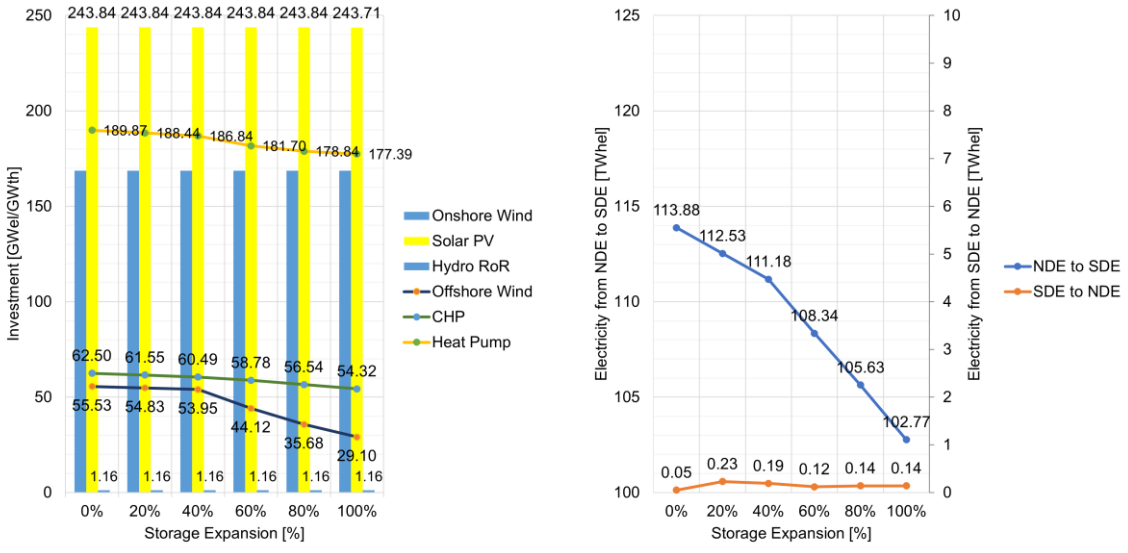

(a) (b)

Figure 23: Effect of storage expansion from current capacity (0%) to double capacity (100%) (a) investment in electricity and heat generators. The varying values of offshore wind, CHP and heat pumps are shown using lines, and the steady onshore wind, solar PV and hydro ROR capacities are shown using columns (b) total annual electrical energy transfer between NDE and SDE. Two different vertical axes are used for showing the exchange, the primary vertical one (left) for NDE to SDE, and the secondary vertical one (right) for SDE to NDE.

Nevertheless, considering the limited reserve capacity of cobalt and vanadium, expanding the battery capacities is a matter of further investigation. The sensitivity analysis for storage expansion also reveals the usage of Hydrogen storages in three instances (0%, 20%, and 40%) when the grid capacity was comparatively low (20 GW_{el}, which is low in comparison with the base, conservative and progressive scenario capacities), and the

other storage options were not sufficient. This result indicates the possibility of Hydrogen storage as another plausible alternative, especially for local energy systems, when other resources for batteries are not adequate, and when the grid expansion is limited. In addition to H_2 storage, the use of Norwegian large hydro capacities is another promising storage option for the future German energy system. Nevertheless, this requires additional investment in interconnection capacities between Norway and Germany and is subject to policy discussions between them.

7. Conclusion

The analysis shows that a 100% renewable energy system for both power and (building) heat sectors are feasible for moderate (progressive) to extreme (conservative) scenario considerations. For onshore wind and hydro ROR investments, maximum potentials should be utilized to meet the demand. In contrast, in the case of PV and offshore wind turbines, the investment capacities depend upon variation in electricity and heat demand, transmission grid expansion, available biomass potential, and storage provisions. The energy mix of such a system is composed of all the possible volatile generator resources, biomass resources, and the already existing renewable capacities. For electrical storage, pumped hydro, ACAES, and batteries are preferred over Hydrogen as storage options.

In volatile generator investments, the scenario analysis shows that a fixed investment of 168.69 GW_{el} onshore wind and 1.16 GW_{el} hydro ROR plants are necessary, along with varying investments of 26.13 – 76.94 GW_{el} offshore wind and 172 – 243.84 GW_{el} solar PV capacities for the three developed scenarios. Onshore wind plants require the maximum annual investment is required (9.84 bn €/yr), and hydro ROR plants require minimum annual investment (0.19 bn €/yr), while offshore wind and solar PV requires varying investments in different scenarios (3.8 – 11.2 bn €/yr for offshore wind and 3.79 – 5.37 bn €/yr for solar PV). The total cost for the volatile generators in Germany, therefore, can vary in between 17.62 bn €/yr and 26.6 bn €/yr, which sums up to 312 – 450 bn € over the lifetime.

Heat generator capacities vary for CHPs between 58.26 GW_{th} and 73.62 GW_{th}, while the heat pump acts as a more preferred alternative heating option for buildings, requiring 154.93 – 181.86 GW_{th} installations for Germany. The cost varies accordingly, for CHPs in between 7.39 bn €/yr and 9.34 bn €/yr, and the heat pumps in between 16.28 bn €/yr and 19.44 bn €/yr. The total cost for the heat generators in Germany, therefore, varies in between 23.67 bn €/yr and 28.78 bn €/yr, which sums up to 316 – 385 bn € over the lifetime.

For storages, while partial investment is suggested for ACAES varying from 0.15 GW_{el} to 0.51 GW_{el}, batteries are preferred over Hydrogen storages for all three scenarios. Existing PHS and ACAES capacities are used throughout the year, and the TES are utilized to their maximum exogenous capacities. The total cost of power and storage shows that maximum investment is required for Li-ion batteries (1.57 bn €/yr), and TES storage capacities (1.1 – 2.21 bn €/yr). With minimum storage provision in the conservative scenario and maximum storage provision in the progressive scenario, the total cost for electrical and heat storages in Germany varies in between 2.67 bn €/yr (conservative) and 3.86 bn €/yr (progressive), which sums up to around 33 – 48 bn € over the full lifetime.

The energy mix comparison with the Fraunhofer Study suggests that a transformation towards 100%-system according to the results from the OSeEM-DE model is feasible by 2050, where the energy mix consists of onshore wind, solar PV, offshore wind, CHP, and hydro ROR plants. The biomass-CHP is a promising option to replace the 15% fossil-fuel-based generation of the 85% system of the Fraunhofer study, and the optimized results from the OSeEM-DE model shows that the German potential is sufficient to meet this requirement. The LCOE results from the OSeEM-DE model have been compared with another Fraunhofer study, which shows that the values are close to each other, except for biomass, which is higher in the OSeEM-DE results because of high biomass cost.

The flexibility of the system was examined via sensitivity analysis of the grid and storage capacities. It is observed that with grid expansion, the cost of offshore wind, solar PV, and heat pump decreases, but the CHP investment increases slightly. On the other hand, with the gradual expansion of storage, offshore wind, CHP, and heat pump investment, and the amount of energy transfer from NDE to SDE decreases. Therefore, maximum utilization of the storage usage and optimum grid expansion can provide additional flexibility to the system and decrease the overall investment cost. The cost of grid expansion vs. investment in generation and storage facilities must be investigated to reach the optimum solution. The limited capacity of battery materials should also be taken into consideration. A possible alternative storage solution is Norwegian hydro storages with the interconnection between Norway and Germany, which is subject to further investigation.

There are several limitations of the developed model and scenarios. Firstly, the transmission grids were modeled as transshipment capacities between two nodes only, which does not reflect the realistic power system. Therefore, the investment cost for the grid expansion could not be estimated and presented in the paper. Secondly, the heating sector does not include industrial heating demand (i.e., process heat). Thirdly, Concentrated Solar Power (CSP) and other renewable-based plants (such as geothermal) were not included in the optimization. The inclusion of these components can ease the need for only CHP and heat pumps as heat generators and cover a portion of the electricity demand. However, since process heating is also excluded in this model, these two renewable options are likely to play a vital role in meeting partial process heating demand. Fourthly, the storage of synthetic gas produced by renewable electricity in P2G converters was not considered in the model. Finally, the import and export of electricity between countries, which is an essential part of the combined energy transition towards the climate-neutrality of the EU, was not considered in the model.

Nonetheless, the developed open modeling tool OSeEM-DE paves the pathway towards modeling and analyzing plausible sector-coupled scenarios for 100% renewable-based national and sub-national energy systems, especially in the NS region. At the same time, this study shows how different energy mix options and their component-wise investment capacities and costs can be investigated using the model; hence the case of Germany can be followed for other similar regions to conduct the feasibility analysis of 100% renewable-based sector-coupled systems. Moreover, the study also reveals that sensitivity analyses can help in identifying the flexibility aspects of the system in future energy infrastructure. On this background, the following plans are outlined for future steps of this research-

1. Integration of the German transport sector, with a particular focus on electric vehicles as dispatchable loads;
2. Inclusion of industrial heating demand, and other possible renewable resources, and demand-side management (DSM) potentials in the German energy sector;
3. Interconnection between the neighboring countries of Germany and analyze the impact of grid exchange in the EU context;
4. Inclusion of Norwegian pumped hydro storage and investigation into its possible consequences;
5. Replication and enhancement of the current model for other areas of the NS region.

Data: Data, source codes, and results of the model is available in the following Github repository:

github.com/znes/OSeEM-DE

Funding: This research is a part of the ENSYSTRA project which received funding from the European Union's Horizon 2020 research and innovation programme under the Marie Skłodowska-Curie grant agreement No: 765515

Acknowledgments: This work was supported by the ENSYSTRA network and by the Center for Sustainable Energy Systems (ZNES) by Europa-Universität Flensburg and the Flensburg University of Applied Sciences. The author would like to thank the Openmod Community and Oemof developers for spreading the idea of open-data and open-science in energy system modeling. The author acknowledges the supervision, guidance and support from Prof. Dr. Olav Hohmeyer, Prof. Dr. Bernd Möller, Dr. Fredrik Hedenus, Simon Hilpert, and Martin Söthe throughout the project.

Conflicts of Interest: The author declares no conflict of interest.

Appendix A

The input data for cost calculation are obtained from various project databases [90–97, 101–102], which are summarized in Table A.1

Table A.1. Input Cost Data for OSeEM-DE Model

	Onshore Wind	**Offshore Wind**	**Solar PV**	**Hydro (ROR)**	**Biomass**	**Li-ion**	**H_2**	**Redox**	**PHS**	**ASHP**	**GSHP**	**ACAES**	**TES**
Capex (€/kW)	1075	2093	425	3000	1951	35	1000	600	2000	1050	1400	750	0
Lifetime (Years)	25	25	25	50	30	20	22.5	25	50	20	20	30	30

WACC	0.025	0.048	0.02	0.05	0.027	0.05	0.05	0.05	0.05	0.05	0.05	0.05	0.05
Variable O&M Cost (€/MWh)	0	0	0	0	11.3	1	1	1	0	0	0	1	0
Fixed O&M Cost (€/kWh)	35	80	25	60	100	10	10	10	20	36.75	49	10	0.38
Storage Capacity Cost (€/kWh)	-	-	-	-	-	187	0.2	70	-	-	-	40	38
Carrier Cost (€/MWh)	-	-	-	-	34.89	-	-	-	-	-	-	-	-

References

[1] European Commission, UN Climate talks: EU plays instrumental role in making the Paris Agreement operational, (2018). https://ec.europa.eu/commission/presscorner/detail/en/IP_18_6824 (accessed August 20, 2020).

[2] European Commission, 2050 long-term strategy, Clim. Action. (2020). https://ec.europa.eu/clima/policies/strategies/2050_en (accessed August 20, 2020).

[3] M.N.I. Maruf, Sector Coupling in the North Sea Region—A Review on the Energy System Modelling Perspective, Energies. 12 (2019) 4298. https://doi.org/10.3390/en12224298

[4] BMUB, Climate Action Plan 2050 – Principles and goals of the German government's climate policy, (2016). https://www.bmu.de/fileadmin/Daten_BMU/Pools/Broschueren/klimaschutzplan_2050_en_bf.pdf (accessed September 23, 2020).

[5] T.W. Brown, T. Bischof-Niemz, K. Blok, C. Breyer, H. Lund, B.V. Mathiesen, Response to 'Burden of proof: A comprehensive review of the feasibility of 100% renewable-electricity systems,' Renew. Sustain. Energy Rev. 92 (2018) 834–847. https://doi.org/10.1016/j.rser.2018.04.113.

[6] M. Robinius, A. Otto, P. Heuser, L. Welder, K. Syranidis, D.S. Ryberg, T. Grube, P. Markewitz, R. Peters, D. Stolten, Linking the Power and Transport Sectors—Part 1: The Principle of Sector Coupling, Energies. 10 (2017) 956. https://doi.org/10.3390/en10070956.

[7] BMWi, Green Paper on Energy Efficiency, (2016). https://www.bmwi.de/Redaktion/EN/Publikationen/green-paper-on-energy-efficiency.pdf (accessed September 23, 2020).

[8] Energiewende hinges on unblocking the power grid, Clean Energy Wire. (2015). https://www.cleanenergywire.org/dossiers/energy-transition-and-germanys-power-grid (accessed August 20, 2020).

[9] Bundesnetzagentur, Netzausbau - Leitungsvorhaben, (2020). https://www.netzausbau.de/leitungsvorhaben/de (accessed September 23, 2020).

[10] BMWi, Using renewable energy efficiently: harnessing flexibility and sector coupling, Sinteg. (2019). https://www.sinteg.de/en/specific-topics/flexibility-and-sector-coupling (accessed September 23, 2020).

[11] A. Blakers, B. Lu, M. Stocks, 100% renewable electricity in Australia, Energy. 133 (2017) 471–482. https://doi.org/10.1016/j.energy.2017.05.168.

[12] O. Hohmeyer, A 100% renewable Barbados and lower energy bills, Europa-Universität Flensburg, Center for Sustainable Energy Systems (CSES), Flensburg, Germany, 2015. https://www.uni-flensburg.de/fileadmin/content/abteilungen/industrial/dokumente/downloads/veroeffentlichungen/diskussionsbeitraege/znes-discussionspapers-005-barbados.pdf (accessed September 22, 2020).

[13] L. de Souza Noel Simas Barbosa, J.F. Orozco, D. Bogdanov, P. Vainikka, C. Breyer, Hydropower and Power-to-gas Storage Options: The Brazilian Energy System Case, Energy Procedia. 99 (2016) 89–107. https://doi.org/10.1016/j.egypro.2016.10.101.

[14] B. Kroposki, B. Johnson, Y. Zhang, V. Gevorgian, P. Denholm, B.-M. Hodge, B. Hannegan, Achieving a 100% Renewable Grid: Operating Electric Power Systems with Extremely High Levels of Variable Renewable Energy, IEEE Power Energy Mag. 15 (2017) 61–73. https://doi.org/10.1109/MPE.2016.2637122.

[15] M. Child, C. Breyer, Vision and initial feasibility analysis of a recarbonised Finnish energy system for 2050, Renew. Sustain. Energy Rev. 66 (2016) 517–536. https://doi.org/10.1016/j.rser.2016.07.001.

[16] M. Huber, C. Weissbart, On the optimal mix of wind and solar generation in the future Chinese power system, Energy. 90 (2015) 235–243. https://doi.org/10.1016/j.energy.2015.05.146.

[17] G. Krajačić, N. Duić, Z. Zmijarević, B.V. Mathiesen, A.A. Vučinić, M. da Graça Carvalho, Planning for a 100% independent energy system based on smart energy storage for integration of renewables and CO2 emissions reduction, Appl. Therm. Eng. 31 (2011) 2073–2083. https://doi.org/10.1016/j.applthermaleng.2011.03.014.

[18] B.V. Mathiesen, H. Lund, D. Connolly, H. Wenzel, P.A. Østergaard, B. Möller, S. Nielsen, I. Ridjan, P. Karnøe, K. Sperling, F.K. Hvelplund, Smart Energy Systems for coherent 100% renewable energy and transport solutions, Appl. Energy. 145 (2015) 139–154. https://doi.org/10.1016/j.apenergy.2015.01.075.

[19] A. Palzer, H.-M. Henning, A comprehensive model for the German electricity and heat sector in a future energy system with a dominant contribution from renewable energy technologies – Part II: Results, Renew. Sustain. Energy Rev. 30 (2014) 1019–1034. https://doi.org/10.1016/j.rser.2013.11.032.

[20] H.-M. Henning, A. Palzer, A comprehensive model for the German electricity and heat sector in a future energy system with a dominant contribution from renewable energy technologies—Part I: Methodology, Renew. Sustain. Energy Rev. 30 (2014) 1003–1018. https://doi.org/10.1016/j.rser.2013.09.012.

[21] S. Pfenninger, J. Keirstead, Renewables, nuclear, or fossil fuels? Scenarios for Great Britain's power system considering costs,

emissions and energy security, Appl. Energy. 152 (2015) 83–93. https://doi.org/10.1016/j.apenergy.2015.04.102.
[22] A. Aslani, M. Naaranoja, K.-F.V. Wong, Strategic analysis of diffusion of renewable energy in the Nordic countries, Renew. Sustain. Energy Rev. 22 (2013) 497–505. https://doi.org/10.1016/j.rser.2013.01.060.
[23] A. Gulagi, D. Bogdanov, C. Breyer, The role of storage technologies in energy transition pathways towards achieving a fully sustainable energy system for India, J. Energy Storage. 17 (2018) 525–539. https://doi.org/10.1016/j.est.2017.11.012.
[24] A. Gulagi, P. Choudhary, D. Bogdanov, C. Breyer, Electricity system based on 100% renewable energy for India and SAARC, PLOS ONE. 12 (2017) e0180611. https://doi.org/10.1371/journal.pone.0180611.
[25] A. Aghahosseini, D. Bogdanov, N. Ghorbani, C. Breyer, Analysis of 100% renewable energy for Iran in 2030: integrating solar PV, wind energy and storage, Int. J. Environ. Sci. Technol. 15 (2018) 17–36. https://doi.org/10.1007/s13762-017-1373-4.
[26] D. Connolly, B.V. Mathiesen, A technical and economic analysis of one potential pathway to a 100% renewable energy system, Int. J. Sustain. Energy Plan. Manag. 1 (2014) 7–28. https://doi.org/10.5278/ijsepm.2014.1.2.
[27] F. Meneguzzo, R. Ciriminna, L. Albanese, M. Pagliaro, Italy 100% Renewable: A Suitable Energy Transition Roadmap, ArXiv160908380 Phys. (2016). http://arxiv.org/abs/1609.08380 (accessed September 22, 2020).
[28] B. Ćosić, G. Krajačić, N. Duić, A 100% renewable energy system in the year 2050: The case of Macedonia, Energy. 48 (2012) 80–87. https://doi.org/10.1016/j.energy.2012.06.078.
[29] A. Sadiqa, A. Gulagi, C. Breyer, Energy transition roadmap towards 100% renewable energy and role of storage technologies for Pakistan by 2050, Energy. 147 (2018) 518–533. https://doi.org/10.1016/j.energy.2018.01.027.
[30] L. Fernandes, P. Ferreira, Renewable energy scenarios in the Portuguese electricity system, Energy. 69 (2014) 51–57. https://doi.org/10.1016/j.energy.2014.02.098.
[31] U. Caldera, D. Bogdanov, S. Afanasyeva, C. Breyer, Role of Seawater Desalination in the Management of an Integrated Water and 100% Renewable Energy Based Power Sector in Saudi Arabia, Water. 10 (2018) 3. https://doi.org/10.3390/w10010003.
[32] O. Hohmeyer, A 100% renewable Seychelles, Europa-Universität Flensburg, Center for Sustainable Energy Systems (CSES), Flensburg, Germany, 2017. https://www.uni-flensburg.de/fileadmin/content/abteilungen/industrial/dokumente/downloads/veroeffentlichungen/diskussionsbeitraege/znes-discussionpapers-008-100ee-mahe.pdf (accessed September 22, 2020).
[33] B.-M.S. Hodge, H. Jain, C. Brancucci, G.-S. Seo, M. Korpås, J. Kiviluoma, H. Holttinen, J.C. Smith, A. Orths, A. Estanqueiro, L. Söder, D. Flynn, T.K. Vrana, R.W. Kenyon, B. Kroposki, Addressing technical challenges in 100% variable inverter-based renewable energy power systems, WIREs Energy Environ. 9 (2020) e376. https://doi.org/10.1002/wene.376.
[34] A. Kilickaplan, D. Bogdanov, O. Peker, U. Caldera, A. Aghahosseini, C. Breyer, An energy transition pathway for Turkey to achieve 100% renewable energy powered electricity, desalination and non-energetic industrial gas demand sectors by 2050, Sol. Energy. 158 (2017) 218–235. https://doi.org/10.1016/j.solener.2017.09.030.
[35] M. Child, C. Breyer, D. Bogdanov, H.-J. Fell, The role of storage technologies for the transition to a 100% renewable energy system in Ukraine, Energy Procedia. 135 (2017) 410–423. https://doi.org/10.1016/j.egypro.2017.09.513.
[36] U.B. Akuru, I.E. Onukwube, O.I. Okoro, E.S. Obe, Towards 100% renewable energy in Nigeria, Renew. Sustain. Energy Rev. 71 (2017) 943–953. https://doi.org/10.1016/j.rser.2016.12.123.
[37] M.J. Alexander, P. James, N. Richardson, Energy storage against interconnection as a balancing mechanism for a 100% renewable UK electricity grid, IET Renew. Power Gener. 9 (2014) 131–141. https://doi.org/10.1049/iet-rpg.2014.0042.
[38] A. Hooker-Stroud, P. James, T. Kellner, P. Allen, Toward understanding the challenges and opportunities in managing hourly variability in a 100% renewable energy system for the UK, Carbon Manag. 5 (2014) 373–384. https://doi.org/10.1080/17583004.2015.1024955.
[39] M.J. Alexander, P. James, Role of distributed storage in a 100% renewable UK network, Proc. Inst. Civ. Eng. - Energy. (2015). https://doi.org/10.1680/ener.14.00030.
[40] A.E. MacDonald, C.T.M. Clack, A. Alexander, A. Dunbar, J. Wilczak, Y. Xie, Future cost-competitive electricity systems and their impact on US CO 2 emissions, Nat. Clim. Change. 6 (2016) 526–531. https://doi.org/10.1038/nclimate2921.
[41] H. Lund, B.V. Mathiesen, Energy system analysis of 100% renewable energy systems—The case of Denmark in years 2030 and 2050, Energy. 34 (2009) 524–531. https://doi.org/10.1016/j.energy.2008.04.003.
[42] B. Elliston, M. Diesendorf, I. MacGill, Simulations of scenarios with 100% renewable electricity in the Australian National Electricity Market, Energy Policy. 45 (2012) 606–613. https://doi.org/10.1016/j.enpol.2012.03.011.
[43] M. Esteban, J. Portugal-Pereira, B.C. Mclellan, J. Bricker, H. Farzaneh, N. Djalilova, K.N. Ishihara, H. Takagi, V. Roeber, 100% renewable energy system in Japan: Smoothening and ancillary services, Appl. Energy. 224 (2018) 698–707. https://doi.org/10.1016/j.apenergy.2018.04.067.
[44] S. Zapata, M. Castaneda, M. Jimenez, A. Julian Aristizabal, C.J. Franco, I. Dyner, Long-term effects of 100% renewable generation on the Colombian power market, Sustain. Energy Technol. Assess. 30 (2018) 183–191. https://doi.org/10.1016/j.seta.2018.10.008.
[45] D. Devogelaer, D. Gusbin, J. Duerinck, W. Nijs, Y. Marenne, M. Orsini, M. Pairon, Towards 100% renewable energy in Belgium by 2050, VITO, Mol (Belgium), Netherlands, 2012. http://www.vito.be/NR/rdonlyres/A75FFE2E-2191-46BD-A6B7-7C640CFB543C/0/130419_Backcasting_FinalReport.pdf (accessed September 22, 2020).
[46] V. Krakowski, E. Assoumou, V. Mazauric, N. Maïzi, Reprint of Feasible path toward 40–100% renewable energy shares for power supply in France by 2050: A prospective analysis, Appl. Energy. 184 (2016) 1529–1550. https://doi.org/10.1016/j.apenergy.2016.11.003.
[47] H.C. Gils, S. Simon, R. Soria, 100% Renewable Energy Supply for Brazil—The Role of Sector Coupling and Regional Development, Energies. 10 (2017) 1859. https://doi.org/10.3390/en10111859.
[48] I.G. Mason, S.C. Page, A.G. Williamson, A 100% renewable electricity generation system for New Zealand utilising hydro, wind, geothermal and biomass resources, Energy Policy. 38 (2010) 3973–3984. https://doi.org/10.1016/j.enpol.2010.03.022.
[49] B.V. Mathiesen, H. Lund, K. Karlsson, 100% Renewable energy systems, climate mitigation and economic growth, Appl. Energy. 88 (2011) 488–501. https://doi.org/10.1016/j.apenergy.2010.03.001.
[50] D. Connolly, H. Lund, B.V. Mathiesen, M. Leahy, The first step towards a 100% renewable energy-system for Ireland, Appl. Energy. 88 (2011) 502–507. https://doi.org/10.1016/j.apenergy.2010.03.006.
[51] H. Lund, Renewable Energy Systems: A Smart Energy Systems Approach to the Choice and Modeling of 100% Renewable Solutions, Academic Press, 2014.
[52] K. Hansen, B.V. Mathiesen, I.R. Skov, Full energy system transition towards 100% renewable energy in Germany in 2050, Renew. Sustain. Energy Rev. 102 (2019) 1–13. https://doi.org/10.1016/j.rser.2018.11.038.
[53] C. Breyer, D. Bogdanov, A. Gulagi, A. Aghahosseini, L.S.N.S. Barbosa, O. Koskinen, M. Barasa, U. Caldera, S. Afanasyeva, M. Child, J. Farfan, P. Vainikka, On the role of solar photovoltaics in global energy transition scenarios, Prog. Photovolt. Res. Appl. 25 (2017) 727–745. https://doi.org/10.1002/pip.2885.
[54] C. Breyer, D. Bogdanov, A. Aghahosseini, A. Gulagi, M. Child, A.S. Oyewo, J. Farfan, K. Sadovskaia, P. Vainikka, Solar photovoltaics demand for the global energy transition in the power sector, Prog. Photovolt. Res. Appl. 26 (2018) 505–523. https://doi.org/10.1002/pip.2950.

[55] M.Z. Jacobson, M.A. Delucchi, Z.A.F. Bauer, S.C. Goodman, W.E. Chapman, M.A. Cameron, C. Bozonnat, L. Chobadi, H.A. Clonts, P. Enevoldsen, J.R. Erwin, S.N. Fobi, O.K. Goldstrom, E.M. Hennessy, J. Liu, J. Lo, C.B. Meyer, S.B. Morris, K.R. Moy, P.L. O'Neill, I. Petkov, S. Redfern, R. Schucker, M.A. Sontag, J. Wang, E. Weiner, A.S. Yachanin, 100% Clean and Renewable Wind, Water, and Sunlight All-Sector Energy Roadmaps for 139 Countries of the World, Joule. 1 (2017) 108–121. https://doi.org/10.1016/j.joule.2017.07.005.

[56] M.Z. Jacobson, M.A. Delucchi, M.A. Cameron, B.V. Mathiesen, Matching demand with supply at low cost in 139 countries among 20 world regions with 100% intermittent wind, water, and sunlight (WWS) for all purposes, Renew. Energy. 123 (2018) 236–248. https://doi.org/10.1016/j.renene.2018.02.009.

[57] D. Bogdanov, C. Breyer, North-East Asian Super Grid for 100% renewable energy supply: Optimal mix of energy technologies for electricity, gas and heat supply options, Energy Convers. Manag. 112 (2016) 176–190. https://doi.org/10.1016/j.enconman.2016.01.019.

[58] M. Huber, A. Roger, T. Hamacher, Optimizing long-term investments for a sustainable development of the ASEAN power system, Energy. 88 (2015) 180–193. https://doi.org/10.1016/j.energy.2015.04.065.

[59] G.C. Czisch, Scenarios for a Future Electricity Supply: Cost-optimized variations on supplying Europe and its neighbours with electricity from renewable energies, IET Digital Library, 2011. https://doi.org/10.1049/PBRN010E.

[60] F. Steinke, P. Wolfrum, C. Hoffmann, Grid vs. storage in a 100% renewable Europe, Renew. Energy. 50 (2013) 826–832. https://doi.org/10.1016/j.renene.2012.07.044.

[61] M.G. Rasmussen, G.B. Andresen, M. Greiner, Storage and balancing synergies in a fully or highly renewable pan-European power system, Energy Policy. 51 (2012) 642–651. https://doi.org/10.1016/j.enpol.2012.09.009.

[62] S. Hagspiel, C. Jägemann, D. Lindenberger, T. Brown, S. Cherevatskiy, E. Tröster, Cost-optimal power system extension under flow-based market coupling, Energy. 66 (2014) 654–666. https://doi.org/10.1016/j.energy.2014.01.025.

[63] D. Connolly, H. Lund, B.V. Mathiesen, Smart Energy Europe: The technical and economic impact of one potential 100% renewable energy scenario for the European Union, Renew. Sustain. Energy Rev. 60 (2016) 1634–1653. https://doi.org/10.1016/j.rser.2016.02.025.

[64] C. Bussar, P. Stöcker, Z. Cai, L. Moraes, R. Alvarez, H. Chen, C. Breuer, A. Moser, M. Leuthold, D.U. Sauer, Large-scale Integration of Renewable Energies and Impact on Storage Demand in a European Renewable Power System of 2050, Energy Procedia. 73 (2015) 145–153. https://doi.org/10.1016/j.egypro.2015.07.662.

[65] G. Pleßmann, P. Blechinger, Outlook on South-East European power system until 2050: Least-cost decarbonization pathway meeting EU mitigation targets, Energy. 137 (2017) 1041–1053. https://doi.org/10.1016/j.energy.2017.03.076.

[66] W.D. Grossmann, I. Grossmann, K.W. Steininger, Solar electricity generation across large geographic areas, Part II: A Pan-American energy system based on solar, Renew. Sustain. Energy Rev. 32 (2014) 983–993. https://doi.org/10.1016/j.rser.2014.01.003.

[67] Z. Bačelić Medić, B. Ćosić, N. Duić, Sustainability of remote communities: 100% renewable island of Hvar, J. Renew. Sustain. Energy. 5 (2013) 041806. https://doi.org/10.1063/1.4813000.

[68] W. Brittlebank, Two German states hit 100% renewable electricity - Climate Action, Clim. Action. (2016). http://www.climateaction.org/news/two_german_states_hit_100_renewable_electricity (accessed September 22, 2020).

[69] H.M. Marczinkowski, P.A. Østergaard, Evaluation of electricity storage versus thermal storage as part of two different energy planning approaches for the islands Samsø and Orkney, Energy. 175 (2019) 505–514. https://doi.org/10.1016/j.energy.2019.03.103.

[70] H.C. Gils, S. Simon, Carbon neutral archipelago – 100% renewable energy supply for the Canary Islands, Appl. Energy. 188 (2017) 342–355. https://doi.org/10.1016/j.apenergy.2016.12.023.

[71] K. Hansen, C. Breyer, H. Lund, Status and perspectives on 100% renewable energy systems, Energy. 175 (2019) 471–480. https://doi.org/10.1016/j.energy.2019.03.092.

[72] E. Schmid, B. Knopf, A. Pechan, Putting an energy system transformation into practice: The case of the German Energiewende, Energy Res. Soc. Sci. 11 (2016) 263–275. https://doi.org/10.1016/j.erss.2015.11.002.

[73] H. Lehmann, M. Nowakowski, Archetypes of a 100% Renewable Energies Power Supply, Energy Procedia. 57 (2014) 1077–1085. https://doi.org/10.1016/j.egypro.2014.10.093.

[74] M. Robinius, A. Otto, K. Syranidis, D.S. Ryberg, P. Heuser, L. Welder, T. Grube, P. Markewitz, V. Tietze, D. Stolten, Linking the Power and Transport Sectors—Part 2: Modelling a Sector Coupling Scenario for Germany, Energies. 10 (2017) 957. https://doi.org/10.3390/en10070957.

[75] A.T. Gullberg, D. Ohlhorst, M. Schreurs, Towards a low carbon energy future – Renewable energy cooperation between Germany and Norway, Renew. Energy. 68 (2014) 216–222. https://doi.org/10.1016/j.renene.2014.02.001.

[76] R. Scholz, M. Beckmann, C. Pieper, M. Muster, R. Weber, Considerations on providing the energy needs using exclusively renewable sources: Energiewende in Germany, Renew. Sustain. Energy Rev. 35 (2014) 109–125. https://doi.org/10.1016/j.rser.2014.03.053.

[77] A. Schroeder, P.-Y. Oei, A. Sander, L. Hankel, L.C. Laurisch, The integration of renewable energies into the German transmission grid—A scenario comparison, Energy Policy. 61 (2013) 140–150. https://doi.org/10.1016/j.enpol.2013.06.006.

[78] W. Nijs, I.H. González, S. Paardekooper, JRC-EU-TIMES and EnergyPLAN comparison, JRC, Petten , Netherlands, 2018. https://heatroadmap.eu/wp-content/uploads/2018/10/D6.3-Methodology-report-for-comparing-the-JRC-EU-TIMES-and-EnergyPLAN-scenarios.pdf (accessed August 21, 2020).

[79] Hilpert, S., Günther, S., Söthe, M., Oemof Tabular, Europa-Universität Flensburg, Flensburg, Germany, 2020. https://github.com/oemof/oemof-tabular (accessed July 8, 2020).

[80] DeStatis, David Liuzzo, Map of Germany, 2006. https://commons.wikimedia.org/wiki/File:Karte_Bundesrepublik_Deutschland.svg (accessed September 22, 2020).

[81] S. Hilpert, Effects of Decentral Heat Pump Operation on Electricity Storage Requirements in Germany, Energies. 13 (2020) 2878. https://doi.org/10.3390/en13112878.

[82] E. Mollenhauer, A. Christidis, G. Tsatsaronis, Evaluation of an energy- and exergy-based generic modeling approach of combined heat and power plants, Int. J. Energy Environ. Eng. 7 (2016) 167–176. https://doi.org/10.1007/s40095-016-0204-6.

[83] T. Brown, D. Schlachtberger, A. Kies, S. Schramm, M. Greiner, Synergies of sector coupling and transmission reinforcement in a cost-optimised, highly renewable European energy system, Energy. 160 (2018) 720–739. https://doi.org/10.1016/j.energy.2018.06.222.

[84] F. Wiese, I. Schlecht, W.-D. Bunke, C. Gerbaulet, L. Hirth, M. Jahn, F. Kunz, C. Lorenz, J. Mühlenpfordt, J. Reimann, W.-P. Schill, Open Power System Data – Frictionless data for electricity system modelling, Appl. Energy. 236 (2019) 401–409. https://doi.org/10.1016/j.apenergy.2018.11.097.

[85] ENTSO-e, Power Statistics, (2020). https://www.entsoe.eu/data/power-stats (accessed July 17, 2020).

[86] O. Ruhnau, When2Heat Heating Profiles, (2019). https://doi.org/10.25832/WHEN2HEAT/2019-08-06.

[87] O. Ruhnau, L. Hirth, A. Praktiknjo, Time series of heat demand and heat pump efficiency for energy system modeling, Sci. Data. 6 (2019) 189. https://doi.org/10.1038/s41597-019-0199-y.

[88] S. Pfenninger, I. Staffell, Renewables.ninja, (2020). https://www.renewables.ninja (accessed July 22, 2020).

[89] K. Kavvadias, I. Hidalgo Gonzalez, A. Zucker, S. Quoilin, Dispa-SET, Energy Modelling Toolkit, 2020. https://github.com/energy-

modelling-toolkit/Dispa-SET (accessed July 22, 2020).
[90] AEE, Facts and Figures on the Development of Renewable Energies in Individual Federal States, (2020). https://www.foederal-erneuerbar.de/landesinfo/bundesland (accessed July 22, 2020).
[91] Deutsche WindGuard GmbH, (2020). https://www.windguard.de (accessed July 22, 2020).
[92] S. Osorio, R. Pietzcker, O. Tietjen, Documentation of LIMES-EU - A long-term electricity system model for Europe, (2020) 93.
[93] T. Brown, J. Hörsch, D. Schlachtberger, PyPSA: Python for Power System Analysis, J. Open Res. Softw. 6 (2018) 4. https://doi.org/10.5334/jors.188.
[94] CSES, ZNES Datapackages, GitHub. (2020). https://github.com/ZNES-datapackages (accessed August 13, 2020).
[95] D.P. Schlachtberger, T. Brown, M. Schäfer, S. Schramm, M. Greiner, Cost optimal scenarios of a future highly renewable European electricity system: Exploring the influence of weather data, cost parameters and policy constraints, Energy. 163 (2018) 100–114. https://doi.org/10.1016/j.energy.2018.08.070.
[96] D.P. Schlachtberger, T. Brown, S. Schramm, M. Greiner, The benefits of cooperation in a highly renewable European electricity network, Energy. 134 (2017) 469–481. https://doi.org/10.1016/j.energy.2017.06.004.
[97] CSES, Input Data for the ANGUSII Project, (2020). https://github.com/ZNES-datapackages/angus-input-data (accessed August 6, 2020).
[98] C. Scaramuzzino, G. Garegnani, Hotmaps Project Data on Potential Biomass - NUTS3 Level, (2020). https://gitlab.com/hotmaps/potential/potential_biomass (accessed July 22, 2020).
[99] P. Ralon, M. Taylor, A. Ilas, Electricity storage and renewables: Costs and markets to 2030, IRENA, Abu Dhabi, UAE, 2017. https://www.irena.org/publications/2017/Oct/Electricity-storage-and-renewables-costs-and-markets (accessed September 23, 2020).
[100] The World Bank, Electric power transmission and distribution losses, (2018). https://data.worldbank.org/indicator/EG.ELC.LOSS.ZS (accessed July 16, 2020).
[101] H.-M. Henning, A. Palzer, What will the energy transformation cost?, Fraunhofer ISE, Germany, 2015. https://www.ise.fraunhofer.de/content/dam/ise/en/documents/publications/studies/What-will-the-energy-transformation-cost.pdf (accessed August 27, 2020).
[102] C. Kost, S. Shammugam, V. Jülch, H.-T. Nguyen, T. Schlegl, Levelized Cost of Electricity- Renewable Energy Technologies, Fraunhofer ISE, Germany, 2020. https://www.ise.fraunhofer.de/en/publications/studies/cost-of-electricity (accessed September 23, 2020).
[103] K. Hedegaard, M. Münster, Influence of individual heat pumps on wind power integration – Energy system investments and operation, Energy Convers. Manag. 75 (2013) 673–684. https://doi.org/10.1016/j.enconman.2013.08.015.